JOC The Journal of Organic Chemistry

Article

pubs.acs.org/joc

Cross-Conjugated Systems Based On An (*E*)-Hexa-3-en-1,5-diyne-3,4-diyl Skeleton: Spectroscopic and Spectroelectrochemical Investigations

Josef B. G. Gluyas,[‡] Valentina Manici,[†] Simon Gückel,[∥] Kevin B. Vincent,[†] Dmitry S. Yufit,[†] Judith A. K. Howard,[†] Brian W. Skelton,[§] Andrew Beeby,[†] Martin Kaupp,[∥] and Paul J. Low*[,‡]

[‡]School of Chemistry and Biochemistry and [§]Centre for Microscopy Characterization and Analysis, University of Western Australia, 35 Stirling Highway, Crawley, Perth 6009, Australia

[†]Department of Chemistry, University of Durham, South Road, Durham DH1 3LE, United Kingdom

[∥]Institut für Chemie, Technische Universität Berlin, Sekr. C7, Strasse des 17. Juni 135, 10623 Berlin, Germany

Supporting Information

ABSTRACT: A series of cross-conjugated compounds based on an (*E*)-4,4′-(hexa-3-en-1,5-diyne-3,4-diyl)bis(*N*,*N*-bis(4-methoxyphenyl)aniline) skeleton (**1**−**6**) have been synthesized. The linear optical absorption properties can be tuned by modification of the substituents at the 1 and 5 positions of the hexa-3-en-1,5-diynyl backbone (**1**: $Si(CH(CH_3)_2)_3$, **2**: $C_6H_4C{\equiv}CSi(CH_3)_3$, **3**: $C_6H_4COOCH_3$, **4**: $C_6H_4CF_3$, **5**: $C_6H_4C{\equiv}N$, **6**: $C_6H_4C{\equiv}CC_5H_4N$), although attempts to introduce electron-donating ($C_6H_4CH_3$, $C_6H_4OCH_3$, $C_6H_4Si(CH_3)_3$) substituents at these positions were hampered by the ensuing decreased stability of the compounds. Spectroelectrochemical investigations of selected examples, supported by DFT-based computational studies, have shown that one- and two-electron oxidation of the 1,2-bis(triarylamine)ethene fragment also results in electronic changes to the perpendicular π-system in the hexa-3-en-1,5-diynyl branch of the molecule. These properties suggest that (*E*)-hexa-3-en-1,5-diynyl-based compounds could have applications in molecular sensing and molecular electronics.

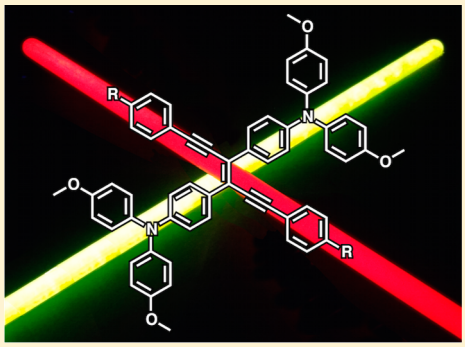

INTRODUCTION

Cruciform and other cross-shaped molecules have attracted interest in recent years due to the fact that the HOMO and LUMO associated with cross-conjugated architectures can be selectively and independently localized to a single one of the constituent linearly conjugated pathways or delocalized over the entire molecule, through judicious choice of both the composition of the cross-conjugated backbone and the electronic nature of substituents.[1] The spatial separation of the HOMO and LUMO that can be engineered in a cross-conjugated system can be exploited to allow independent control of both the HOMO−LUMO gap and intramolecular charge-transfer (ICT) pathways within the cross-conjugated framework.[2] This property is particularly useful in the design of photoresponsive or electro-active materials for sensing applications, as recognition elements can be incorporated into the peripheral groups of the cross-conjugated core, leading to molecules where chemical binding of an analyte will result in specific and independent changes to the optical and electronic response.[3,4] These unique properties have sparked interest in materials of this type and prompted the investigation of a variety of compounds based on an idealized X-shaped architecture. Structures include those based on spirocycles,[5,6] tetraethynylethenes,[7,8] 1,2,4,5-tetraethynyl benzenes,[9−11] and tetrasubstituted distyryl benzenes (cruciforms).[3] Additionally, cross-conjugated compounds have recently been investigated in the context of organic[12,13] and molecular electronics.[14−18] For example, cross-conjugated carotenoids have recently been shown to display altered electronic conductance properties in response to changes in the electron-withdrawing nature of the cross-conjugated substituents,[19] and other systems serve as models through which to explore the concepts of quantum interference and molecular switching in single molecule electronics.[15,18,20−23] We report herein on the synthesis of cross-conjugated donor−acceptor systems based on the (*E*)-hexa-3-en-1,5-diyne skeleton and the investigation of their electronic and structural properties as a prelude to further studies of systems of this type in single molecule electronic junctions.

RESULTS AND DISCUSSION

Syntheses. The key step in the synthesis of the cross-conjugated target compounds **1**−**6** was the formation of the hexa-3-en-1,5-diyne backbone. This was achieved by dimerization of propargyl bromides **7** and **8** (Scheme 1) utilizing the LiHMDS/HMPA-mediated carbenoid coupling−elimination strategy first described by Jones.[24] Initially, trialkylsilylacetylenes **11** and **12** were lithiated with *n*-butyl lithium and reacted with 4-bromobenzaldehyde to afford propargyl alcohols **13**[25] and **14** (52%). Reaction of **13** and **14** with freshly prepared

Received: September 25, 2015
Published: October 23, 2015

ACS Publications © 2015 American Chemical Society

DOI: 10.1021/acs.joc.5b02240
J. Org. Chem. 2015, 80, 11501−11512

Scheme 1. Synthesis of the Cross-Conjugated (*E*)-Hexa-3-en-1,5-diyne Backbone

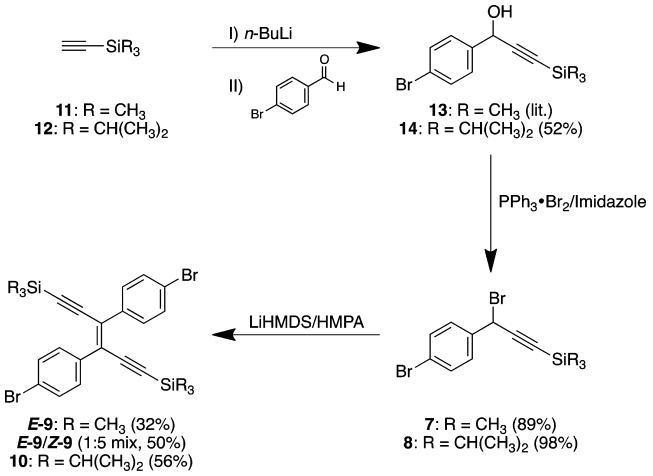

triphenylphosphine bromide complex furnished **7** (89%) and **8** (98%). By ensuring a high degree of purity in propargyl alcohols **13** and **14**, both propargyl bromides **7** and **8** could be obtained in sufficient purity to be used directly in subsequent reactions; attempts at further purification of **7** and **8** resulted in decomposition of the reactive propargyl bromides. Dimerization of **7** using Jones' method[24] was essentially nonregiospecific and afforded a mixture of both possible isomers of the trimethylsilyl substituted compound **9** with an *E*/*Z* ratio of 65:35 (by ^{1}H NMR) in the crude product. Separation of the desired *E*-**9** from *Z*-**9** was hindered by their very similar polarities, and chromatography gave only a low yield of *E*-**9** (32%) and a 1:5 mixture (by ^{1}H NMR) of *E*-**9** and *Z*-**9** (50%). In addition, *E*-**9** proved to be incompatible with subsequent Buchwald–Hartwig amination reaction conditions (Δ ∼ 100 °C, NaO^{t}Bu)[26,27] (c.f. Scheme 2), presumably with cleavage of the C–Si bonds resulting in a competing homocoupling or thermal polymerization of the now exposed terminal alkyne moieties; *E*-**9** also decomposes on prolonged storage. Tuning of the *E*/*Z* selectivity of the carbenoid coupling methodology can be achieved by modification of the steric bulk and, to a lesser extent, electronic properties, of substituents on the propargyl bromide backbone.[24] In light of this, and since the triisopropylsilylethynyl group has far greater stability toward basic conditions than the trimethylsilylethynyl moiety,[28] compound **8** was selected as a substrate. Thus, the *E* configured triisopropylsilyl substituted hexa-3-en-1,5-diyne (**10**) was synthesized in 56% yield from **8** (Scheme 1).

Buchwald–Hartwig[26,27] coupling of the cross-conjugated (*E*)-hexa-3-en-1,5-diyne building block **10** with bis(4-methoxyphenyl)amine (**15**) was employed to produce the cross-conjugated diamine **1** in 60% yield (Scheme 2). From **1** a two pot-two step (**2**) or one pot-two step (**3** − **6**) sequence of desilylation and Sonogashira cross-coupling reactions[29−31] with appropriate aryl iodides furnished a small library of triarylamine donor–aryl acceptor molecules based on *para*-substituted aromatic moieties pendent to the (*E*)-hexa-3-en-1,5-diyne core (Scheme 2). Compound **6** could alternatively be synthesized from **2** in 90% yield via a one pot-two step sequence of desilylation and Sonogashira cross-coupling with 4-iodopyridine. All of the (*E*)-hexa-3-en-1,5-diyne-based compounds (**1**–**6**, *E*-**9**, **10**) were obtained isomerically pure, as determined by ^{1}H NMR spectroscopy. Single crystal X-ray diffraction (XRD) studies of

Scheme 2. Synthesis of Cross-Conjugated Bis-Triphenylamine Compounds

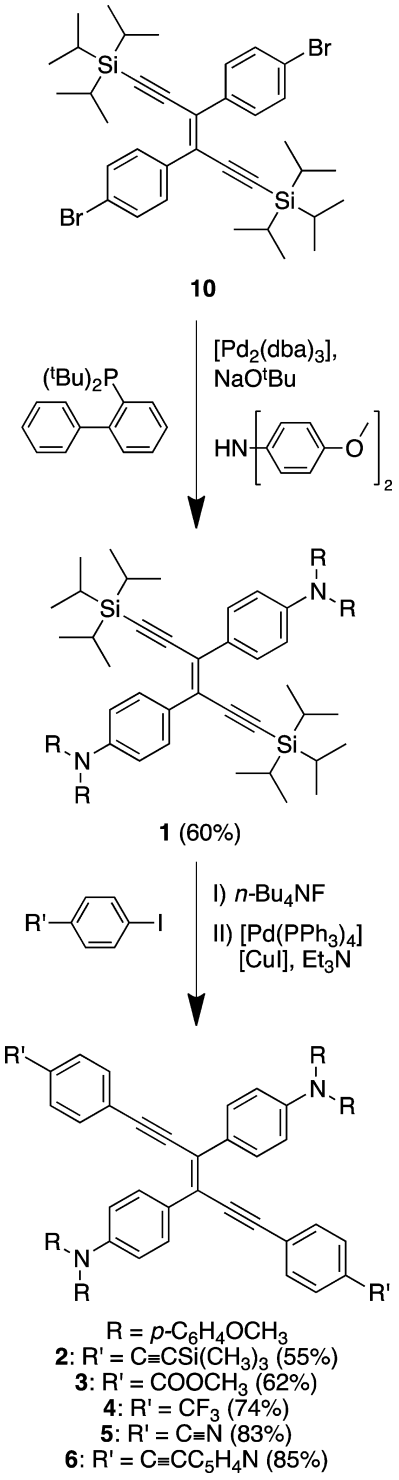

1, **6**, *E*-**9**, and **10** served to confirm the assignment of this compound family as the desired *E* isomers (see Supporting Information (SI)). Compounds **2** and **6** incorporate trimethylsilylethynyl[32,33] and pyridyl[34−36] moieties which can function as surface binding groups so as to allow future investigation of this class of compounds in single molecule conductance experiments.[18,21] However, attempts to react **1** with aryl iodides containing even modestly electron-donating groups to create donor–donor systems, via a one pot-two step

DOI: 10.1021/acs.joc.5b02240
J. Org. Chem. 2015, 80, 11501−11512

sequence of desilylation and Sonogashira cross coupling analogously to that described for the synthesis of **2**–**6**, for example, through reactions of **1** with 4-iodotoluene, 4-iodoanisole, or 4-iodo(trimethylsilyl)benzene,[37] failed.

Electrochemical Properties. The presence of the two triarylamine fragments in **1**–**6** prompted investigation of the electrochemical response of these compounds.[38] In dichloromethane/0.1 M NBu_4PF_6 solution, the cyclic voltammogram of each of **1**–**6** was characterized by two overlapped, unresolved one-electron oxidation processes, giving rise to a wave with ΔE_p varying from 70 mV (indicating two almost completely independent redox processes) for **2** to 140 mV for **1** (more consistent with two overlapping processes), which compare with ΔE_p = 70 and 80 mV, respectively (Table 1) for the internal decamethylferrocene standard.[39] The electrochemical processes were largely chemically reversible, and the apparent half-wave potential of the detectable forward and reverse peak potentials of the amine-based oxidations were modestly sensitive to the electronic character of the remote aryl substituent (Table 1). The nitrile substituted complex **5** exhibited the most positive apparent $E_{1/2}$ value (+260 mV vs $FeCp_2/[FeCp_2]^+$), while **2**, which features the much more weakly electron-withdrawing C≡CSiMe$_3$ substituent, gave an apparent $E_{1/2}$ of +205 mV under the same conditions. The overlapping voltammetric waves in the compounds **1**–**6** compare with the ca. 140 mV separation of the two redox processes ($\Delta E_{1/2}$) in the model bis(diarylamino)stilbene **16** (Chart 1).[40,41] The relationship between $\Delta E_{1/2}$ in E-bridge-E compounds (where E = electrophore) and the electronic structure of the intermediate, mixed-valence compound $[E\text{-bridge-}E]^{+\bullet}$ has been discussed and debated elsewhere,[38,42−44] and we will return to this point in the discussion of electronic structure below.

Table 1. Cyclic Voltammetry Data for Compounds 1–6 in 0.1 M *n*-Bu_4NPF_6/Dichloromethane Relative to $FeCp_2/[FeCp_2]^+$ ($E_{1/2}$ = 0.00 V)[39]

	$E_{1/2}$ (mV)	ΔEp (mV)	Fc*ΔEp (mV)	ip_c/ip_a
1	225	140	80	0.97
2	205	70	70	0.88
3	240	110	70	0.93
4	240	100	95	0.95
5	260	105	90	0.94
6	200	75	65	1.00

Chart 1. Model Bis(diarylamino)stilbenes

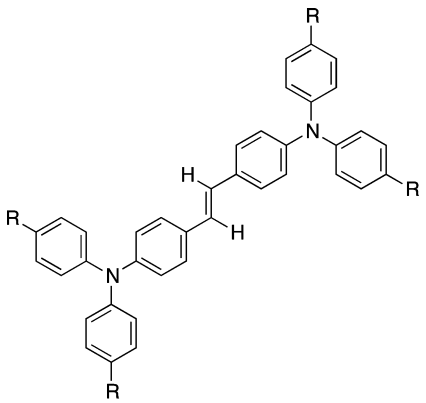

16: R = OMe
17: R = H

Structure Optimizations. In order to support the spectral investigations and further explore the electronic structure of these redox-active, cross-conjugated ene-diynes, DFT and time-dependent density functional theory (TDDFT) calculations were carried out on the neutral complexes **1** and **3** and also on the somewhat simplified model complex $[\mathbf{1'}]^+$ in which the Si^{i}Pr$_3$ moieties were replaced by SiMe$_3$ groups. All calculations were carried out using the global hybrid functional BLYP35, the def2-TZVP basis set, and a suitable dielectric continuum solvent model (dichloromethane), see Computational Details below. This computational protocol has been specifically developed to properly characterize mixed-valence systems[45,46] and was used also for the neutral complexes **1** and **3** to maintain consistency.

Optimization of **1** and **3** gave structures that were in excellent agreement with the available crystallographically determined data (Table 2 and SI). The structures were optimized without symmetry constraints, and the structural variations between the chemically identical parts of each molecule are trivially small. The most significant differences between these calculated and crystallographically determined structures are associated with the pitch of the aryl moieties in the propeller-like triarylamine fragments, the crystallographic structures displaying generally smaller pitch, presumably to better accommodate packing in the solid state. In each case, the HOMO is essentially localized along the bis(diarylamino)stilbene fragment, with the LUMO more heavily associated with the hexa-3-en-1,5-diyne moiety (Figure 1).

Table 2. Selected Bond Lengths (Å) from the Optimized Geometries of 1, $[\mathbf{1'}]^+$, and 3 and Crystallographically Determined Data From 1

	1 (X-ray)	**1** (DFT)	$[\mathbf{1'}]^+$ (DFT)	**3** (DFT)
C1−C1′	1.365(4)	1.359		1.368
C1−C1a			1.376	
C1−C2	1.440(3)	1.419	1.418	1.415
C1a-C2a			1.420	
C2−C3	1.204(3)	1.208	1.208	1.204
C2a-C3a			1.208	
C3−Si1	1.840(2)	1.837	1.841	
C3a-Si1a			1.843	
C1−C4	1.488(3)	1.484	1.471	1.482
C1a-C4a			1.469	
C7−N1	1.405(3)	1.401	1.396	1.397
C7a-N1a			1.385	
N1−C19	1.437(3)	1.417	1.403	1.418
N1a-C19a			1.422	
N1−C26	1.428(3)	1.417	1.403	1.419
N1a-C26a			1.422	

Optical Properties. The experimental optical spectra of compounds **1**–**6** (Figure 2, Table 3) are each characterized by one (**1**) or two (**2**–**6**) absorption bands below 370 nm. TDDFT calculations allowed the assignment of the higher energy (**C** Table 3, Figure 1) of these bands to the stilbene-like $\pi-\pi^*$ transition and the lower (**B** Table 3, Figure 1) to the hexa-3-en-1,5-diyne $\pi-\pi^*$ transition. In the case of **1** the hexa-3-en-1,5-diyne $\pi-\pi^*$ is blue-shifted by ca. 50 nm, and so the two $\pi-\pi^*$ features overlap and are indistinguishable in the experimental spectrum. Each spectrum also exhibits a lower energy band between 434 (**1**) and 494 (**5**) nm that can be attributed to a charge-transfer (CT) transition from the bis(amino)stilbene donor fragment to the hexa-3-en-1,5-diyne acceptor (**A** Table 3, Figure 1). These assignments are consistent with the spectra of other bis(diarylamino)stilbenes, such as **16** (Figure S8) and

DOI: 10.1021/acs.joc.5b02240
J. Org. Chem. 2015, 80, 11501−11512

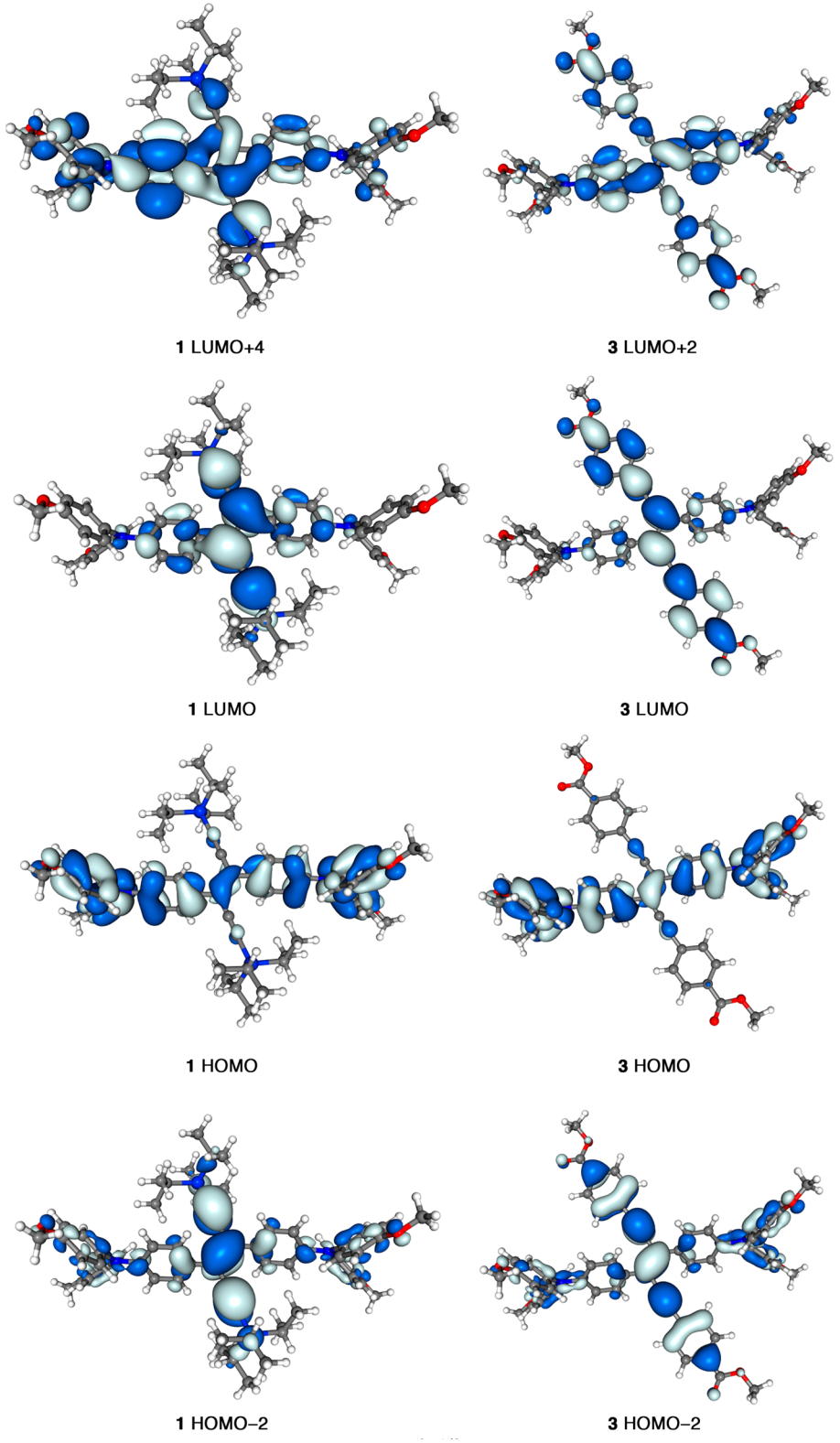

Figure 1. Plots of the orbitals ($\pm$0.02 (e/bohr^3)$^{1/2}$) of **1** (left) and **3** (right) responsible for the spectroscopically observed transitions.

17[47,48] (Chart 1) and *E*-hexa-3-en-1,5-diynes[49] and supported by the results of TDDFT calculations on **1** and **3** (Table 3, Figure S10). The lowest energy absorption band (**A**) displays sensitivity to the electronic nature of the substituent and degree of conjugation in the "acceptor" hexa-3-en-1,5-diyne π-system. Thus, compound **1** featuring the shortest ene-diyne fragment has the highest energy (shortest wavelength) CT transition (434 nm), which shifts to 471−494 nm on introduction of the phenylene moieties in **2**−**6**. Within the series **2**−**6**, the CT energy decreases **2** (C≡CSiMe$_3$) ≈ **4** (CF$_3$) < **3** (CO$_2$Me) < **6** (C≡CC$_5$H$_4$N) < **5** (C≡N), broadly reflecting the electron accepting properties of the aryl substituent.

Upon excitation, compounds **1**−**5** display extremely weak fluorescence at room temperature in 2-methyl THF. However,

DOI: 10.1021/acs.joc.5b02240
J. Org. Chem. 2015, 80, 11501−11512

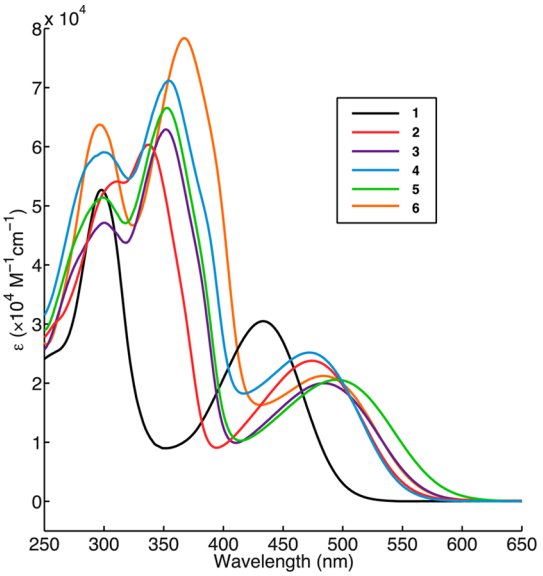

Figure 2. Absorption spectra of **1**−**6** in dichloromethane.

Table 3. Apparent Band Maxima for Absorption (1−6, Dichloromethane, 20 °C) and Fluorescence Spectra (1−5, 2-Methyl THF, −196 °C, Excitation at 350 nm)

	λ_{abs} (nm)			
	A	B	C	λ_{em} (nm)
1[a]	434	297		536
2	471	354	300	579
3[b]	483	352	300	594
4	472	337	309	580
5	494	352	298	604
6	487	367	296	–

[a]TDDFT calculated transitions: **A**, HOMO → LUMO (24967 cm^{-1}; μ_{trans} = 6.9 D); **B**, HOMO−2 → LUMO (32607 cm^{-1}; μ_{trans} = 6.2 D); **C**, HOMO → LUMO+4 (34126 cm^{-1}, μ_{trans} = 6.7). [b]TDDFT calculated transitions: **A**, (HOMO → LUMO, 19662 cm^{-1}, μ_{trans} = 6.9 D); **B**, (HOMO−2 → LUMO, 25682 cm^{-1}, μ_{trans} = 10.8 D); **C**, HOMO → LUMO+2 (30900 cm^{-1}, μ_{trans} = 8.9 D).

at cryogenic temperatures in the same solvent, the fluorescence intensity increases significantly (Figure 3 and Table 3). Irradiation of the solid materials **1**−**5** with a 356 nm UV lamp also gives rise to visible emission (Figure S9). These observations are attributed to the reduction of nonradiative decay in the low temperature glasses and solid state which are promoted by molecular motion in the solution state, sometimes referred to as rigidochromism.[50−52] Each of the compounds **1**−**5** exhibit near-identical band shapes in their emission spectra, the spectrum of **1** also displaying an additional weak band at ca. 400 nm. All the compounds were studied using three different excitation wavelengths (300, 350, and 430 nm (**1**); 300, 350, and 400 nm (**2**−**5**)) in order to elucidate which states contribute to the emission. In each case the profile and λ_{max} of the excitation spectrum proved to be independent of the excitation wavelength. Moreover the good overlap between the excitation and absorption spectra confirms that only the states involved in absorption at room temperature are responsible for the emission observed at cryogenic temperatures and confirm that the observed emission is indeed fluorescence. In addition, the emission spectra of **2**−**5** are significantly red-shifted relative to that of **1**. Similarly to the changes observed in the UV−vis spectra, this red shift of the

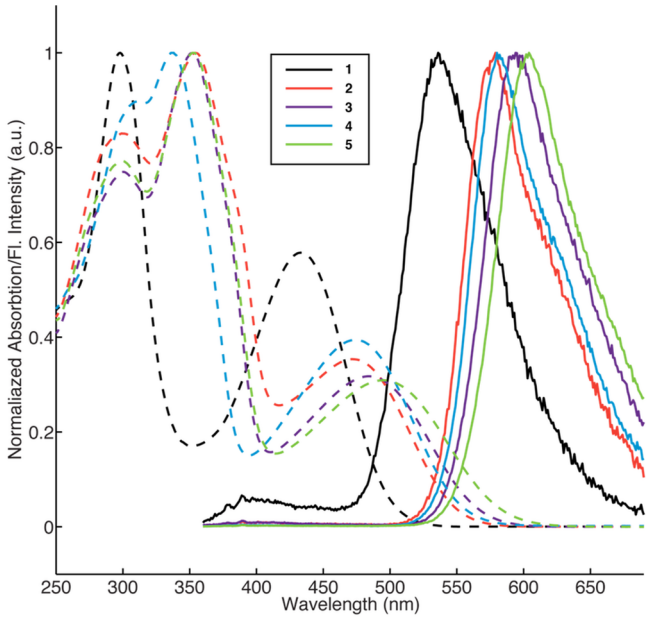

Figure 3. Normalized absorption spectra of **1**−**5** in dichloromethane (dashed lines) and normalized emission spectra of **1**−**5** in 2-methyl THF at −196 °C under 350 nm irradiation (solid lines).

emission spectra also appears to be affected more by the extension of the π-system than the electron-withdrawing effects of the aromatic substituents. For example, the trifluoromethyl (**4**) and cyano (**5**) groups are comparable electron-withdrawing groups with greater electron-withdrawing properties than the methyl ester group in **3**. However, the emission profiles are red-shifted such that the emission maxima fall in the order λ_{em} **4** < **3** < **5** (Table 3, Figure 3). Red shift of emission spectra in molecules of this type is associated with lowering the energy of the LUMO and possibly the introduction of low-lying (perhaps twisted) CT states from which emission occurs.[53]

Spectroelectrochemistry. Compounds **1** and **3** were investigated by IR and UV−vis−NIR spectroelectrochemical methods in order to explore the influence of oxidation on the physical and electronic structure of the cross-conjugated backbone. While **1** is the most structurally simple example, compound **3** was chosen as a representative example from the series **2**−**6** as in addition to the extremely weak ν(C≡C) (**1**, 2130 cm^{-1}; **3**, 2200 cm^{-1}) and stronger aryl ν(C═C) (**1**, 1611sh, 1600; **3** 1613sh, 1603 cm^{-1}) and ν(C−H) (**1**, 1504 cm^{-1}; **3**, 1505 cm^{-1}) bands, **3** offers an additional ester reporting group that gives a distinct, well resolved ν(C═O) band at 1721 cm^{-1} in the IR spectrum.

IR absorption bands in three characteristic regions are shown for both **1** and **3** (ν(C≡C) ∼ 2150 cm^{-1}; ν(C═C) ∼ 1600 cm^{-1}; ν(C−H) ∼ 1500 cm^{-1}), with **3** also exhibiting an ester ν(C═O) band at ∼1700 cm^{-1} (Table 4, Figure 4). Although the comproportionation constants associated with the equilibria

$$\mathbf{1} + [\mathbf{1}]^{2+} \rightleftharpoons 2[\mathbf{1}]^{+}$$

$$\mathbf{3} + [\mathbf{3}]^{2+} \rightleftharpoons 2[\mathbf{3}]^{+}$$

are small and hence spectra collected by spectroelectrochemical means will be a comproportionated mixture of the three redox states, careful monitoring of the 1000−7000 cm^{-1} spectral region allowed spectra containing the maximum equilibrium concentration of the monocations to be obtained, as well as the spectra of the dication following exhaustive electrolysis of

DOI: 10.1021/acs.joc.5b02240
J. Org. Chem. 2015, 80, 11501−11512

Table 4. IR Data (cm^{-1}) Obtained Spectroelectrochemically for Compounds 1 and 3 in Dichloromethane/0.1 M NBu_4PF_6 Using an OTTLE Cell[54]

	ν(C≡C)	ν(C=O)	ν(C=C)	ν(C–H)
1	2130	–	1611(sh)	1504
			1600	
$\mathbf{1}^{+}$	2130	–	1608, 1599	1582
				1505
$\mathbf{1}^{2+}$	2111	–	1601	1503
			1588	
3	2200	1721	1613(sh)	1505
			1603	
$\mathbf{3}^{+}$	2200	1722	1604	1505
	2166		1576	
$\mathbf{3}^{2+}$	2166	1724	1608	1503
			1581	

the solution within the electroactive cell volume (Figure 4, Figure S7). Interestingly, the effects of one-electron oxidation were not confined to the bis(diarylamino)stilbene moiety, with oxidation resulting in a shift of −20 to −35 cm^{-1} in the ν(C≡C) band (most prominent in the series $[\mathbf{3}]^{n+}$) as well as general decreases in the frequency of the aryl ring stretching ν(C=C) and aryl ν(C–H) modes, although the increase in the ν(C=O) band from **3** to $[\mathbf{3}]^{+}$ to $[\mathbf{3}]^{2+}$ spans only 3 cm^{-1}.

The members of the redox series $[\mathbf{1}]^{n+}$ and $[\mathbf{3}]^{n+}$ display broadly similar UV–vis–NIR absorption bands, indicating similar underlying electronic structures (Figure 5), and the spectra of the neutral species have been discussed above. In the comproportionated mixtures of $[\mathbf{1}]^{n+}$ and $[\mathbf{3}]^{n+}$ obtained during electrolysis, a low energy (NIR) band unique to the +1 state was clearly observed ($[\mathbf{1}]^{+}$, 5685 cm^{-1}; $[\mathbf{3}]^{+}$, 5590 cm^{-1}), which collapses on further exhaustive electrolysis to the dications.

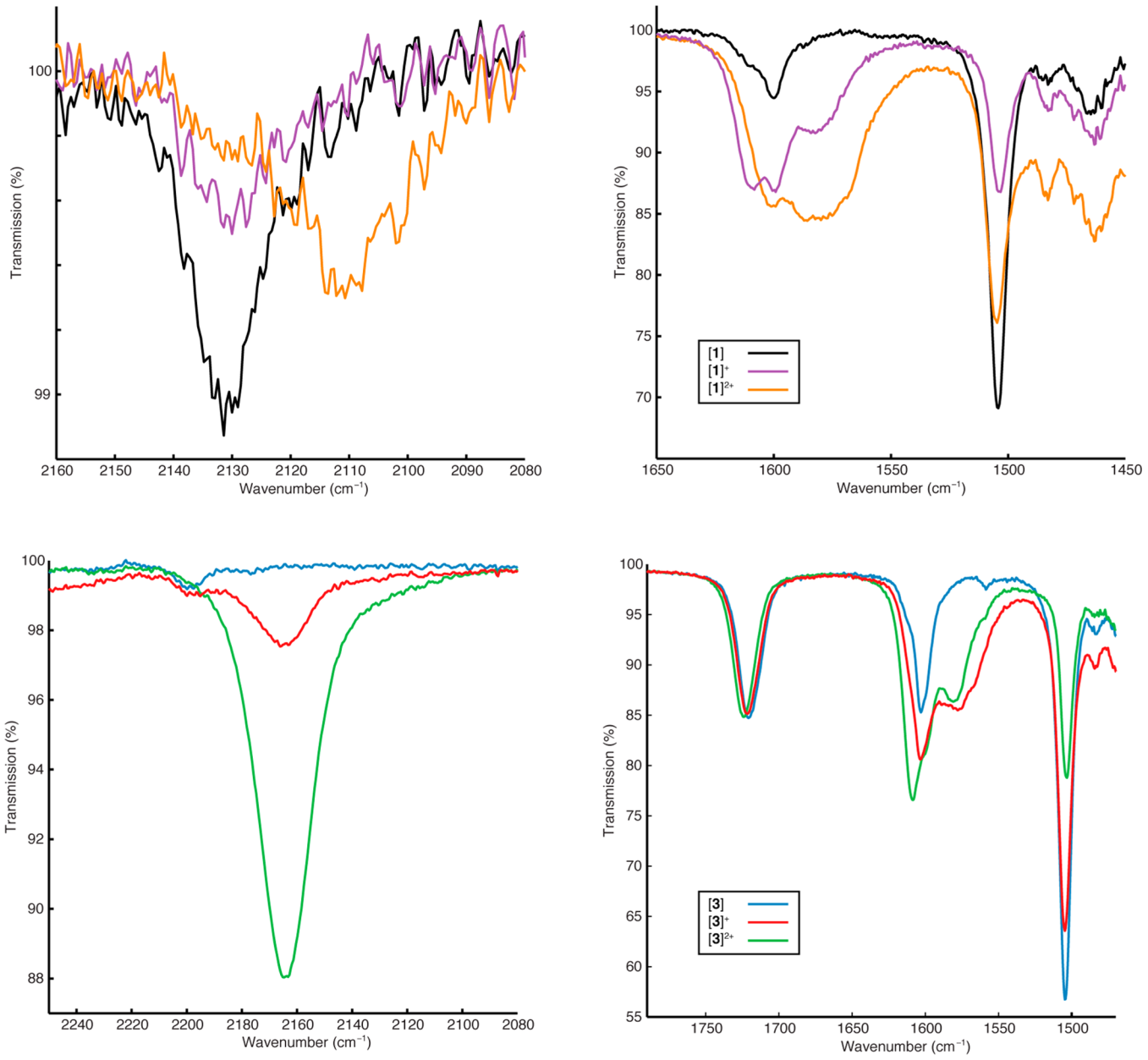

Figure 4. IR data obtained spectroelectrochemically for compounds **1** (upper) and **3** (lower) in dichloromethane/0.1 M NBu_4PF_6 using an OTTLE[54] cell plotted against an arbitrary transmission scale.

DOI: 10.1021/acs.joc.5b02240
J. Org. Chem. 2015, 80, 11501–11512

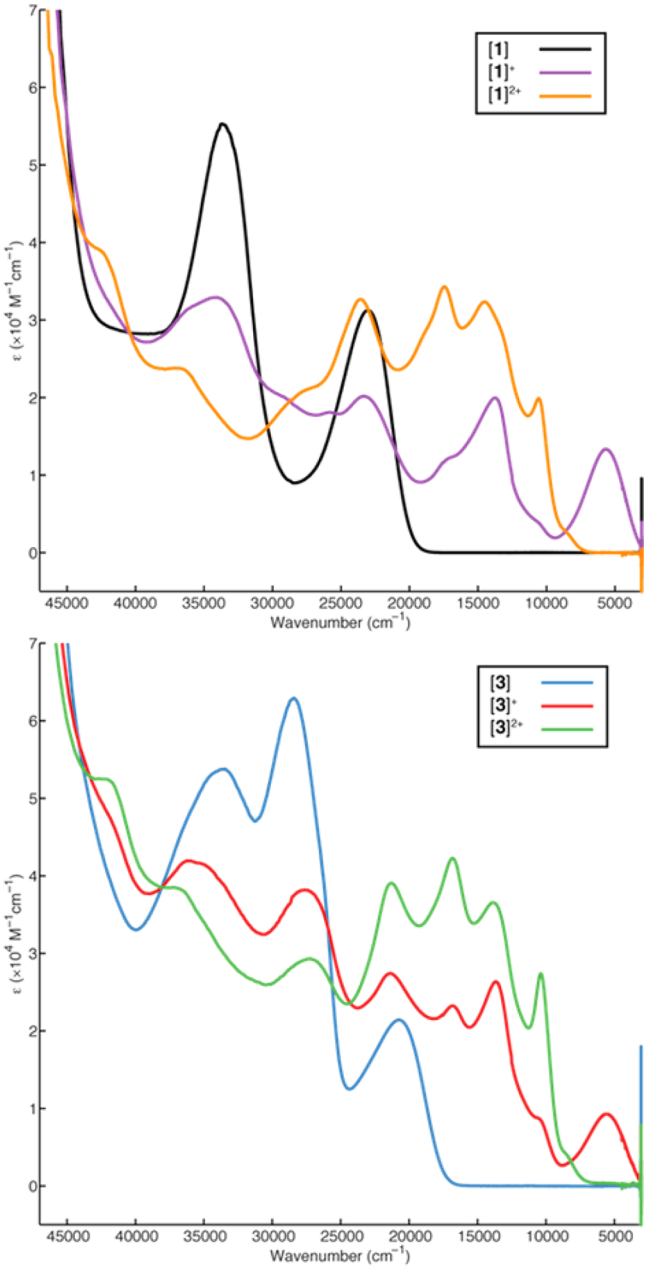

Figure 5. UV−vis-NIR data obtained spectroelectrochemically for compounds **1** (upper) and **3** (lower) in dichloromethane/0.1 M NBu_4PF_6 using an OTTLE[54] cell.

Similar NIR bands are observed in other formally mixed-valent bis(diarylamino)stilbenes,[40,41] and the observation raises the issue of the most appropriate descriptions of the organic mixed-valence systems $[\mathbf{1}]^+$ and $[\mathbf{3}]^+$ in terms of localized or delocalized electronic structures.[38] The parent bis(diarylamino)stilbene $[\mathbf{16}]^+$ has been characterized as a delocalized (Class III mixed valence) radical cation, based on the intensity (ε 39500 M^{-1} cm^{-1}) and asymmetry ($\overline{\nu}_{1/2}$[high]/$\overline{\nu}_{1/2}$[low] = 1.40, where $\overline{\nu}_{1/2}$[high] and $\overline{\nu}_{1/2}$[low] are twice the half-widths on the high and low energy sides of the band) of the NIR (or charge resonance) band, and comparison with the values derived from the Hush relationships from a two-state model.[40,41] In the case of $[\mathbf{1}]^+$ and $[\mathbf{3}]^+$ the degree of coupling is apparently reduced by the introduction of cross-conjugation to the bridging moiety, with the greater symmetry of the NIR bands ($\overline{\nu}_{1/2}$[high]/$\overline{\nu}_{1/2}$[low]: $[\mathbf{1}]^+$, 1.18; $[\mathbf{3}]^+$, 1.22) more consistent with values obtained from the Class II (valence trapped) alkyne bridged analogue $[(MeOC_6H_4)_2NC_6H_4C{\equiv}CC_6H_4N(C_6H_4OMe)_2]^+$ ($[\mathbf{18}]^+$) and lending weight to a better description of the NIR absorption bands in both $[\mathbf{1}]^+$ and $[\mathbf{3}]^+$ as arising from true intervalence charge-transfer (IVCT) transitions.[40,41]

To test the valence-trapped mixed valence description of $[\mathbf{1}]^+$ and $[\mathbf{3}]^+$, the solvatochromic nature of the NIR band was examined. To avoid complications arising from the high ionic strength of the electrolyte solutions, solutions of **1** and **3** in dichloromethane, acetone, and acetonitrile were titrated with $SbCl_5$ (as a 1 M solution in dichloromethane) to give solutions containing the mixed-valence radical cations as the $[SbCl_6]^-$ salts. The significant blue shift of the NIR band (Figure 6) in

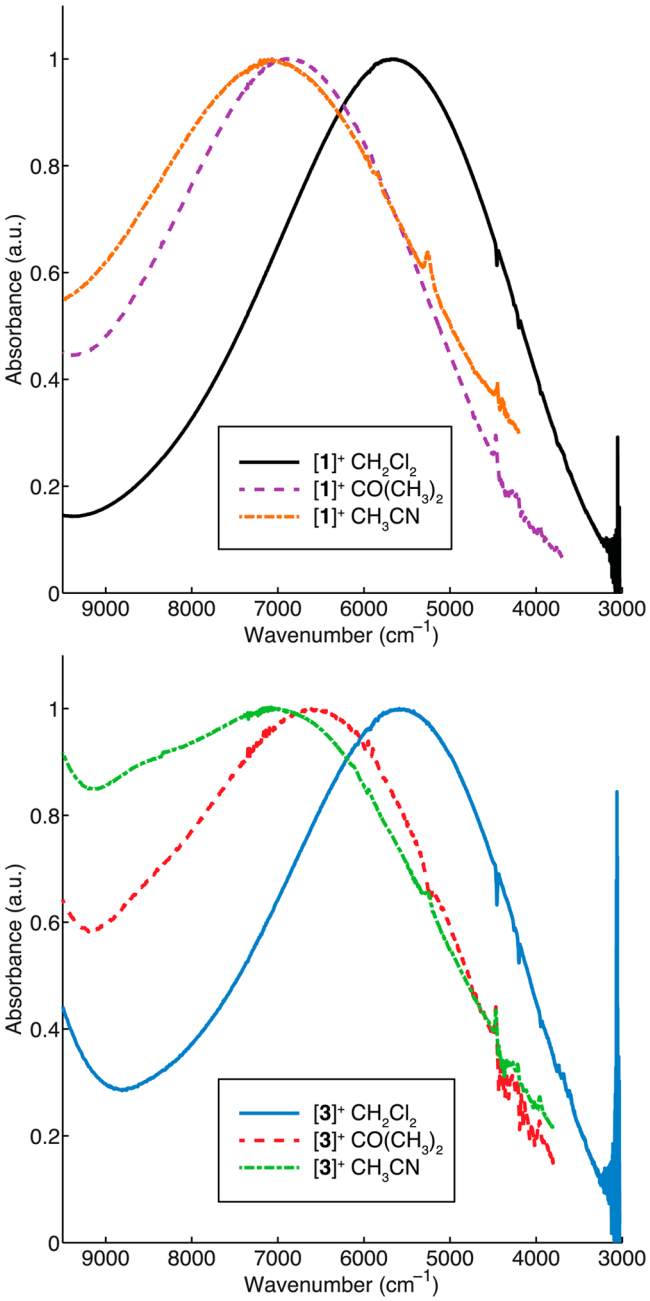

Figure 6. NIR spectra of $[\mathbf{1}]^+$ (upper) and $[\mathbf{3}]^+$ (lower) obtained by titration of **1** and **3**, respectively, with $SbCl_5$ (1 M in dichloromethane) recorded in dichloromethane, acetone, and acetonitrile. The spectra are plotted against an arbitrary absorbance scale.

DOI: 10.1021/acs.joc.5b02240
J. Org. Chem. 2015, 80, 11501−11512

the more polar solvents ($[\mathbf{1}]^+$: dichloromethane 5685 cm^{-1}; acetone 6911 cm^{-1}, acetonitrile 7067 cm^{-1}, $[\mathbf{3}]^+$ dichloromethane 5590 cm^{-1}; acetone 6609 cm^{-1}, acetonitrile 7077 cm^{-1}) is consistent with the ca. 2170 cm^{-1} blue shift in the IVCT band of $[\mathbf{18}]^+$ in dichloromethane (5760 cm^{-1}) versus acetonitrile (7930 cm^{-1}).[40,41] On further oxidation ($[\mathbf{1}]^+ \rightarrow [\mathbf{1}]^{2+}$/$[\mathbf{3}]^+ \rightarrow [\mathbf{3}]^{2+}$) the IVCT band collapses, and the spectral features between 10000−25000 cm^{-1} gain intensity with those associated with the neutral species between 25000−45000 cm^{-1} losing intensity.

The optimized structure of the model complex $[\mathbf{1}']^+$ exhibits a distinctly asymmetric molecular structure, which is most obvious from the elongation of the N−C(aryl) bonds at one nitrogen center (Table 1). Plots of the β-SOMO and β-LUMO are given in Figure 7 and support the localized (Class II)

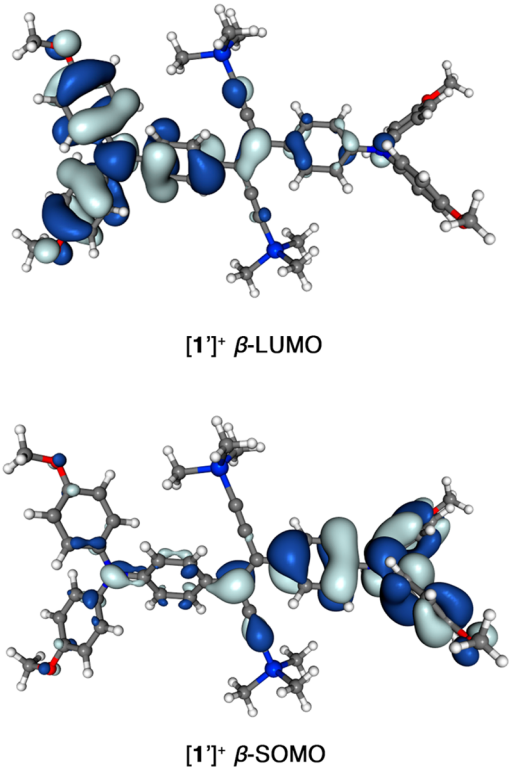

Figure 7. A plot of the β-LUMO (upper) and the β-SOMO of $[\mathbf{1}']^+$ (lower) (±0.02 $(e/bohr^3)^{1/2}$).

electronic structure inferred from the analysis of the NIR band-shape described above. In addition a single IVCT-type transition at 6573 cm^{-1} (β-SOMO→β-LUMO, μ_{trans} = 11.3 D) was calculated for $[\mathbf{1}']^+$ which compares well with the experimentally observed values ($[\mathbf{1}]^+$, 5685 cm^{-1}; $[\mathbf{3}]^+$, 5590 cm^{-1}) and provides additional evidence for the assignment of these complexes as localized mixed valence systems. It therefore appears that in contrast to the parent bis(diarylamino)stilbene radical cation ($[\mathbf{16}]^+$), for which an extensively delocalized electronic structure has been proposed on the basis of both NIR band shape analysis and electronic structure calculation, the introduction of the extended, cross-conjugated molecular backbone leads to a more localized (Class II organic mixed valence) electronic structure.

CONCLUSIONS

A robust synthetic approach to a compact cross-conjugated framework based on an (*E*)-hexa-3-en-1,5-diyne skeleton has been developed. Compounds **1**, **2**, and **10** can function as building blocks for a variety of related compounds being easily functionalized through common palladium-catalyzed cross coupling methods. The electronic and spectroscopic properties of the donor−acceptor 'X' shaped systems **1**−**6** are sensitive to changes in the electronic nature of the substituents along the hexa-3-en-1,5-diyne fragment. In addition the spectroelectrochemical investigations presented herein demonstrate that redox state changes in the bis(amino)stilbene moiety affect the entire cross-conjugated molecular backbone. This property could prove particularly useful in the field of molecular electronics as the wire-like (*E*)-hexa-3-en-1,5-diyne moiety could be "switched" by oxidation or reduction of the triarylamine moieties. Furthermore, the clear presence of three distinct acetylene signals on oxidation of **1** and **3** ($\mathbf{1} \rightarrow \mathbf{1}^+ \rightarrow \mathbf{1}^{2+}$ and $\mathbf{3} \rightarrow \mathbf{3}^+ \rightarrow \mathbf{3}^{2+}$) hints at the possibility of a three-state molecular switch, allowing steps to be taken toward three-step logic in molecular electronics. Investigations into the behavior of compounds **2** and **6** in nanoscale electronic junctions are currently in progress.

EXPERIMENTAL SECTION

General Procedures. All reactions were carried out under dry nitrogen. Reaction workup was carried out in air with no specific precautions against oxygen or moisture, unless otherwise stated. Solvents were either distilled over sodium/benzophenone (tetrahydrofuran) or calcium sulfate (triethylamine) and stored under dry nitrogen, or used as received. The petroleum ether used was from the fraction boiling between 40−60 °C. The compounds $Pd(PPh_3)_4$,[55] $Pd_2(dba)_3$,[56] 4-iodo(trimethylsilylethynyl)benzene,[57] 4-((4-iodophenyl)ethynyl)-pyridine,[58] **13**,[25] **15**,[59] and **16**[40] were synthesized according to literature procedures. Unless otherwise indicated, all other reagents were commercially available and used as received. NMR spectroscopy was carried out using 700, 600, and 400 MHz instruments, and the spectra were referenced relative to internal solvent resonances (^1H and ^{13}C)[60] external $CF_3C_6H_5$ (^{19}F δ = −63.72 ppm) or external tetramethylsilane (^{29}Si δ = 0.0 ppm). Assignment of the ^1H and ^{13}C NMR data was supported by gradient selected ^{13}C, ^1H HMQC and HMBC experiments. FT-IR spectra of solids were recorded from solutions in dichloromethane in a calcium fluoride cell, the FT-IR spectra of oils were recorded neat between sodium chloride discs. Fluorescence spectra were measured in a cylindrical quartz cuvette at 77 K frozen in a glass of 2-methyl tetrahydrofuran and at ambient temperature in the same solvent. Each sample was investigated using three different excitation wavelengths (300, 350, and 430 nm (**1**); 300, 350, and 400 nm (**2**−**5**)). Mass spectrometry was carried out employing ASAP (APCI) or ESI ionization techniques. High-resolution mass spectrometry (HRMS) was carried out using ESI-FTICR or ESI-TOF techniques. UV−vis measurements were performed using solutions in dichloromethane in a 1 mm quartz cuvette. Cyclic voltammetry was carried out with a platinum disc working electrode, a platinum wire counter electrode, and a platinum wire pseudoreference electrode, from solutions in dichloromethane containing 0.1 M NBu_4PF_6 as the electrolyte. Measurements with ν = 100, 200, 400, and 800 $mV \cdot s^{-1}$ showed that the ratio of the anodic to cathodic peak currents varied linearly as a function of the square root of scan rate in all cases. The decamethylferrocene/decamethylferrocinium ($FeCp^*_2/[FeCp^*_2]^+$) couple was used as an internal reference for potential measurements such that the couple falls at −0.55 V relative to external $FeCp_2/[FeCp_2]^+$ at 0.00 V.[61] FT-IR and UV−vis−NIR spectroelectrochemistry was conducted with solutions in dichloromethane containing 0.1 M NBu_4PF_6 as the electrolyte and ∼1 mg/mL of analyte using an OTTLE cell of Hartl[54] design, and electrolysis in the cell was performed using a computer controlled potentiostat.

*(E)-4,4′-(1,6-Bis(tri-isopropylsilyl)hexa-3-en-1,5-diynyl)bis(N,N-bis(4-methoxyphenyl)aniline) (**1**).* A mixture of **10** (2.14 g, 3.07 mmol), **15** (1.39 g, 7.05 mmol), $Pd_2(dba)_3$ (84.0 mg, 9.20 mmol),

DOI: 10.1021/acs.joc.5b02240
J. Org. Chem. 2015, 80, 11501−11512

2-(di-*tert*-butylphosphino)biphenyl (101 mg, 337 μmol), potassium tert-butoxide (1.06 g, 11.0 mmol), and toluene (25 mL) was heated at reflux for 15 h, allowed to cool to ambient temperature, diluted with toluene (20 mL), and filtered. The solvent of the filtrate was removed under reduced pressure, and the resulting brown residue was purified by flash column chromatography (eluent: petroleum ether/ethyl acetate (90:10 (v/v))). Concentration of the appropriate fractions (TLC analysis) gave an orange solid which was dissolved in the minimum volume of dichloromethane and diluted with methanol until solid began to precipitate, sufficient dichloromethane was added to redissolve all the solid, and the solution was cooled to −25 °C overnight affording **1**, as a bright yellow-orange crystalline solid, which was recovered by filtration, in 60% yield (1.82 g, 1.83 mmol). ^{1}H NMR (599.7 MHz $CDCl_3$): δ 1.01−1.02 (m, 42 H, Si(C*H*(CH_3)$_2$), 3.80 (s, 12 H, OCH_3), 6.82−6.85 (m, 12 H, C═C−C_6H_4 and C_6H_4OCH_3), 7.05−7.07 (m, 8 H, C_6H_4OCH_3), 7.73−7.75 (m, 4 H, C═C−C_6H_4). ^{29}Si{^{1}H} NMR (139.0 MHz, $CDCl_3$): δ − 2.5. FT-IR (CH_2Cl_2): ν = 1505 (C−H), 1600 (C═C), 2131 (C≡C). ESI-MS: *m*/*z* (%) 995 (10) [M$^+$], 335 (100). Anal. calcd for $C_{64}H_{78}N_2O_4Si_2$: C, 77.22; H, 7.90; N, 2.81. Found C, 77.20; H, 7.84; N, 2.77. HRMS (ESI-FTICR) *m*/*z*: [M]$^+$ calcd for $C_{64}H_{78}O_4N_2Si_2$ 994.54946; Found 994.55088. Signal broadening affected the NMR characterization of **1** (see ^{1}H NMR spectrum in SI), and a satisfactory ^{13}C{^{1}H} NMR spectrum could not be obtained. This may be due to steric congestion between the triisopropyl silyl and triarylamine groups resulting in restricted rotation about the C−N bond coupled with slow inversion at the nitrogen center. A single crystal of **1** suitable for XRD studies was grown by layer diffusion of ethanol into a solution of **1** in dichloromethane.

*(E)-4,4′-(1,6-Bis(4-((trimethylsilyl)ethynyl)phenyl)hexa-3-en-1,5-diyne-3,4-diyl)bis(N,N-bis(4-methoxyphenyl)aniline) (**2**).* A solution of tetrabutyl ammonium fluoride in tetrahydrofuran (1.0 M, 2.27 mL, 869 μmol of *n*-Bu_4NF) was added to a stirred solution of **1** (393 mg, 395 μmol) in tetrahydrofuran (15 mL). The resulting mixture was stirred for 15 min at ambient temperature and diluted with dichloromethane (30 mL) and water (20 mL), the organic phase was separated, dried over magnesium sulfate, filtered, and concentrated to yield a bright yellow solid. This solid was immediately dissolved in a mixture of dichloromethane (20 mL) and triethylamine (10 mL), and the mixture was sparged with nitrogen for 20 min followed by addition of $Pd(PPh_3)_4$ (16.8 mg, 15.8 μmol), copper(I)iodide (3.00 mg, 15.8 μmol), and 4-iodo(trimethylsilylethynyl)benzene[57] (261 mg, 869 μmol). This mixture was stirred at ambient temperature for 18 h and then concentrated to dryness under reduced pressure. The residue was purified by flash column chromatography (eluent: petroleum ether/ethyl acetate (gradient elution, 90:10 → 80:20 → 70:30 (v/v))). Concentration of the relevant fractions (TLC control) and recrystallization from absolute ethanol afforded **2** as a bright orange microcrystalline solid in 55% yield (224 mg, 218 μmol). ^{1}H NMR (400.1 MHz CD_2Cl_2): δ 0.25 (s, 18 H, Si(CH_3)$_3$), 3.80 (s, 12 H, OCH_3), 6.87 (δ_A) and 7.11 (δ_B) (AA′BB′ system, $^{3}J_{A\text{-}B}$ = 9.4 Hz, $^{4}J_{A\text{-}A',\ B\text{-}B'}$ = 2.2 Hz, 16 H, C_6H_4OCH_3), 6.93 (δ_A) and 7.78 (δ_B) (AA′BB′ system, $^{3}J_{A\text{-}B}$ = 8.4 Hz, $^{4}J_{A\text{-}A',\ B\text{-}B'}$ = 1.6 Hz, 8 H, C_6H_4−C═C), 7.26 (δ_A) and 7.38 (δ_B) (AA′BB′ system, $^{3}J_{A\text{-}B}$ = 8.9 Hz, $^{4}J_{A\text{-}A',\ B\text{-}B'}$ = 1.4 Hz, 8 H, C_6H_4−C≡C). ^{13}C{^{1}H} NMR (100.6 MHz, CD_2Cl_2): δ − 0.06 (Si(CH_3)$_3$), 55.9 (OCH_3), 94.0 (C═C−*C*≡C), 97.0 (Si−*C*≡C), 98.1 (C_6H_4−*C*≡C), 104.8 (C_6H_4−C≡C), 115.1 (C-3/C-5 C_6H_4OCH_3), 119.1 (C-2/C-6, C_6H_4−C═C), 123.4 (C-1 or C-4, C_6H_4−C≡C), 123.9 (C-1 or C-4, C_6H_4−C≡C), 126.9 (C═C), 127.4 (C-2/C-6 C_6H_4OCH_3), 130.3 (C-3/C-5, C_6H_4−C═C), 130.7 (C-4, C_6H_4−C═C), 131.5 (C−H, C_6H_4−C≡C) 132.2 (C−H, C_6H_4−C≡C), 140.9 (C-1 C_6H_4OCH_3), 149.4 (C-1, C_6H_4−C═C), 156.8 (C-4 C_6H_4OCH_3). ^{29}Si{^{1}H} NMR (139.0 MHz, CD_2Cl_2): δ − 17.4. FT-IR (CH_2Cl_2): ν 1505 (C−H), 1602 (C═C), 2149 (C≡C), 2158 (C≡C). APCI-MS: *m*/*z* (%) 1027 (84) [M$^+$], 214 (100). HRMS (ESI-TOF) *m*/*z*: [M + H]$^+$ calcd for $C_{68}H_{63}N_2O_4Si_2$ 1027.4326; Found 1027.4303.

*General Procedure for the Synthesis of **3**−**6**.* A solution of tetrabutyl ammonium fluoride in tetrahydrofuran (1.0 M, 578 μL, 221 μmol of *n*-Bu_4NF) was added to a stirred solution of **1** (100 mg, 100 μmol) in tetrahydrofuran (10 mL). The resulting mixture was stirred for 15 min at ambient temperature and diluted with triethylamine (5 mL), followed by addition of $Pd(PPh_3)_4$ (4.27 mg, 4.02 μmol), copper(I)iodide (1.00 mg, 5.27 μmol) an appropriate 4-iodobenzene derivative (2.2 equiv, 221 μmol), and water (100 μL). This mixture was stirred at ambient temperature for 18 h and then concentrated to dryness under reduced pressure. The residue was dissolved in dichloromethane and precipitated with methanol to afford the product, which was recovered by filtration and dried in air.

*(E)-Dimethyl 4,4′-(3,4-bis(4-(bis(4-methoxyphenyl)amino)-phenyl)hexa-3-en-1,5-diyne-1,6-diyl)dibenzoate (**3**).* Bright red powder 62% (59.0 mg, 62.0 μmol). ^{1}H NMR (400.1 MHz CD_2Cl_2): δ 3.80 (s, 12 H, C_6H_4OCH_3), 3.89 (s, 6 H, COOCH_3), 6.88 (δ_A) and 7.12 (δ_B) (AB system, $^{3}J_{A\text{-}B}$ = 9.5 Hz, 16 H, C_6H_4OCH_3), 6.93 (δ_A) and 7.40 (δ_B) (AB system, $^{3}J_{A\text{-}B}$ = 8.5 Hz, 8 H, C_6H_4−C═C), 7.79 (δ_A) and 7.96 (δ_B) (AB system, $^{3}J_{A\text{-}B}$ = 7.9 Hz, 8 H, C_6H_4COOCH_3). ^{13}C{^{1}H} NMR (100.6 MHz, CD_2Cl_2): δ 52.5 (COOCH_3), 55.9 (OCH_3), 94.8 (C═C−C≡C), 97.8 (C═C−C≡C), 115.1 (C-3/C-5 C_6H_4OCH_3), 119.1 (C-2/C-6, C_6H_4−C═C), 127.3 (C-1, C_6H_4COOCH_3), 127.5 (C-2/C-6 C_6H_4OCH_3), 128.3 (C═C), 129.8 (C−H, C_6H_4COOCH_3), 130.1 (C-4, C_6H_4COOCH_3), 130.4 (C-3/C-5, C_6H_4−C═C), 130.7 (C-4, C_6H_4−C═C), 131.5 (C−H, C_6H_4COOCH_3), 140.8 (C-1 C_6H_4OCH_3), 149.6 (C-1, C_6H_4−C═C), 156.9 (C-4 C_6H_4OCH_3), 166.6 (COOCH_3). FT-IR (CH_2Cl_2): ν 1504 (C−H), 1603 (C═C), 1720 (C═O), 2198 (C≡C). APCI-MS: *m*/*z* (%) 951 (32) [M$^+$], 257 (100). HRMS (ESI-TOF) *m*/*z*: [M]$^+$ calcd for $C_{62}H_{50}N_2O_8$ 950.3567; Found 950.3549.

*(E)-4,4′-(1,6-Bis(4-(trifluoromethyl)phenyl)hexa-3-en-1,5-diyne-3,4-diyl)bis(N,N-bis(4-methoxyphenyl)aniline) (**4**).* Bright red powder 74% (72.3 mg, 74.5 μmol). ^{1}H NMR (400.1 MHz CD_2Cl_2): δ 3.80 (s, 12 H, OCH_3), 6.87 (δ_A) and 7.12 (δ_B) (AA′BB′ system, $^{3}J_{A\text{-}B}$ = 8.7 Hz, $^{4}J_{A\text{-}A',\ B\text{-}B'}$ = 2.9 Hz, 16 H, C_6H_4OCH_3), 6.93 (δ_A) and 7.79 (δ_B) (AA′BB′ system, $^{3}J_{A\text{-}B}$ = 8.4 Hz, $^{4}J_{A\text{-}A',\ B\text{-}B'}$ = 1.9 Hz, 8 H, C_6H_4−C═C), 7.45 (m, 4 H, $C_6H_4CF_3$), 7.57 (m, 4 H, C_6H_4−C≡C). ^{13}C{^{1}H} NMR (100.6 MHz, CD_2Cl_2): δ 55.9 (OCH_3), 94.2 (C═C−C≡C), 97.0 (C═C−C≡C), 115.1 (C-3/C-5 C_6H_4OCH_3), 119.0 (C-2/C-6, C_6H_4−C═C), 124.4 (q, $^{1}J_{C-F}$ = 273 Hz, CF_3), 125.7 (q, $^{3}J_{C-F}$ = 3.7 Hz, C-3/C-5, $C_6H_4CF_3$), 127.2 (C-1, $C_6H_4CF_3$), 127.5 (C-2/C-6 C_6H_4OCH_3), 127.7 (m, C-2/C-6, $C_6H_4CF_3$), 130.2 (C═C), 130.3 (C-3/C-5, C_6H_4−C═C), 131.9 (C-4, C_6H_4−C═C), 140.8 (C-1 C_6H_4OCH_3), 149.6 (C-1, C_6H_4−C═C), 156.9 (C-4 C_6H_4OCH_3), *C*-4 $C_6H_4CF_3$ not observed. ^{19}F NMR (376.5 MHz, CD_2Cl_2): δ −63.1. FT-IR (CH_2Cl_2): ν 1504 (C−H), 1603 (C═C), 2202 (C≡C). APCI-MS: *m*/*z* (%) 971 (100) [M$^+$]. HRMS (ESI-TOF) *m*/*z*: [M]$^+$ calcd for $C_{60}H_{44}F_6N_2O_4$ 970.3205; Found 970.3199.

*(E)-4,4′-(3,4-Bis(4-(bis(4-methoxyphenyl)amino)phenyl)hexa-3-en-1,5-diyne-1,6-diyl)dibenzonitrile (**5**).* Burgandy powder 83% (73.6 mg, 83.0 μmol). ^{1}H NMR (400.1 MHz CD_2Cl_2): δ 3.80 (s, 12 H, C_6H_4OCH_3), 6.88 (δ_A) and 7.12 (δ_B) (AA′BB′ system, $^{3}J_{A\text{-}B}$ = 8.1 Hz, $^{4}J_{A\text{-}A',\ B\text{-}B'}$ = 2.2 Hz, 16 H, C_6H_4OCH_3), 6.92 (δ_A) and 7.75 (δ_B) (AA′BB′ system, $^{3}J_{A\text{-}B}$ = 8.8 Hz, $^{4}J_{A\text{-}A',\ B\text{-}B'}$ = 2.2 Hz, 8 H, C_6H_4−C═C), 7.41 (δ_A) and 7.60 (δ_B) (AA′BB′ system, $^{3}J_{A\text{-}B}$ = 9.2 Hz, $^{4}J_{A\text{-}A',\ B\text{-}B'}$ = 2.2 Hz, 8 H, C_6H_4C≡N). ^{13}C{^{1}H} NMR (100.6 MHz, CD_2Cl_2): δ 55.9 (OCH_3), 95.9 (C≡N), 97.0 (C═C−C≡C), 100.4 (C═C−C≡C), 112.0 (C-4, C_6H_4C≡N), 115.2 (C-3/C-5 C_6H_4OCH_3), 119.1 (C-2/C-6, C_6H_4−C═C), 127.4 (C-1, C_6H_4C≡N), 127.5 (C-2/C-6 C_6H_4OCH_3), 128.4 (C-4, C_6H_4−C═C), 130.0 (C═C), 130.3 (C-3/C-5, C_6H_4−C═C), 132.1 (C−H, C_6H_4C≡N), 132.5 (C−H, C_6H_4C≡N), 140.6 (C-1 C_6H_4OCH_3), 149.7 (C-1, C_6H_4−C═C), 156.9 (C-4 C_6H_4OCH_3). FT-IR (CH_2Cl_2): ν 1505 (C−H), 1602 (C═C), 2200 (C≡C), 2230 (C≡N). ESI-MS: *m*/*z* (%) 884 (75) [M$^+$], 279 (100). HRMS (ESI-FTICR) *m*/*z*: [M]$^+$ calcd for $C_{60}H_{44}N_4O_4$ 884.33571; Found 884.33720.

*(E)-4,4′-(1,6-Bis(4-(pyridin-4-ylethynyl)phenyl)hexa-3-en-1,5-diyne-3,4-diyl)bis(N,N-bis(4-methoxyphenyl)aniline) (**6**).* Bright red powder 85% (88.6 mg, 85.4 μmol). ^{1}H NMR (400.1 MHz CD_2Cl_2): δ 3.80 (s, 12 H, OCH_3), 6.88 (δ_A) and 7.12 (δ_B) (AA′BB′ system, $^{3}J_{A\text{-}B}$ = 8.3 Hz, $^{4}J_{A\text{-}A',\ B\text{-}B'}$ = 2.9 Hz, 16 H, C_6H_4OCH_3), 6.94 (δ_A) and 7.80 (δ_B) (AA′BB′ system, $^{3}J_{A\text{-}B}$ = 8.3 Hz, $^{4}J_{A\text{-}A',\ B\text{-}B'}$ = 1.5 Hz, 8 H, C_6H_4−C═C), 7.35 (δ_A) and 7.51 (δ_B) (AA′BB′ system, $^{3}J_{A\text{-}B}$ = 8.5 Hz, $^{4}J_{A\text{-}A',\ B\text{-}B'}$ = 1.7 Hz, 8 H, C_6H_4−C≡C), 7.39 (m, 4 H, H-3/H-5, C_5H_4N), 8.60 (m, 4 H, H-2/H-6, C_5H_4N). ^{13}C{^{1}H} NMR (100.6 MHz,

DOI: 10.1021/acs.joc.5b02240
J. Org. Chem. 2015, 80, 11501−11512

CD_2Cl_2): δ 55.5 (OCH_3), 88.6 (C═C−C≡C), 93.2 (C_6H_4−C≡C), 94.0 (C_6H_4−C≡C), 97.6 (C_5H_4N−C≡C), 114.7 (C-3/C-5 $C_6H_4OCH_3$), 118.7 (C-2/C-6, C_6H_4−C═C), 121.9 (C-1 or C-4, C_6H_4−C≡C), 124.2 (C-1 or C-4, C_6H_4−C≡C), 125.4 (C-3/C-5 C_5H_4N), 126.6 (C═C), 127.0 (C-2/C-6 $C_6H_4OCH_3$), 129.9 (C-3/C-5, C_6H_4−C═C), 130.2 (C-4, C_6H_4−C═C), 131.2 (C−H, C_6H_4−C≡C) 131.8 (C−H, C_6H_4−C≡C), 140.4 (C-1 $C_6H_4OCH_3$), 149.0 (C-2/C-6 C_5H_4N), 149.9 (C-1, C_6H_4−C═C), 156.4 (C-4 $C_6H_4OCH_3$), C-4 (C_5H_4N) not observed. FT-IR (CH_2Cl_2): ν 1505 (C−H), 1600 (C═C), 2198 (C≡C), 2220 (C≡C). ESI-MS: m/z (%) 1037 (12) $[M + H]^+$, 611 (90), 214 (100). HRMS (ESI-TOF) m/z: $[M + H]^+$ calcd for $C_{72}H_{53}N_4O_4$ 1037. 40613; Found 1037.40651.

*Alternative Synthesis of (E)-4,4′-(1,6-bis(4-(pyridin-4-ylethynyl)-phenyl)hexa-3-en-1,5-diyne-3,4-diyl)bis(N,N-bis(4-methoxyphenyl)-aniline) (**6**).* A solution of tetrabutyl ammonium fluoride in tetrahydrofuran (1.0 M, 588 μL, 225 μmol of n-Bu_4NF) was added to a stirred solution of **2** (100 mg, 97.0 μmol) in tetrahydrofuran (10 mL). The resulting mixture was stirred for 15 min at ambient temperature, and $Pd(PPh_3)_4$ (4.14 mg, 3.89 μmol), copper(I)iodide (1.00 mg, 5.25 μmol), 4-iodopyridine (44.0 mg, 97.0 μmol), and water (100 μL) were added. This mixture was stirred at ambient temperature for 2 h and then concentrated to dryness under reduced pressure. The residue dissolved in dichloromethane (4 mL) and precipitated by addition of methanol (20 mL), and the precipitate was isolated by filtration affording **6** as a bright red powder in 90% yield (90.5 mg, 87.3 μmol). All analytical data were identical to those given above. A single crystal of **6** suitable for XRD studies was grown by slow evaporation of a solution in d_2-dichloromethane.

*(E)-3,4-Bis(4-bromophenyl)-1,6-bis(trimethylsilyl)hexa-3-en-1,5-diyne (E-**9**).* Bromine (1.35 g, 8.47 mmol of Br_2) was added dropwise at 0 °C to a stirred solution of triphenylphosphine (2.32 g, 8.83 mmol) in dichloromethane (27 mL). A solution of compound **13** (2.00 g, 7.06 mmol) and imidazole (577 mg, 8.47 mmol) in dichloromethane (15 mL) was added to the solution of bromine triphenylphosphine complex via cannula at 0 °C. Subsequently, the reaction mixture was allowed to warm to ambient temperature, stirred for 3 h at this temperature, and concentrated *in vacuo*. Diethyl ether (35 mL) was added to the residue, and the flask was placed into an ultrasound bath until a homogeneous beige precipitate in a pale yellow solution was obtained. The precipitate was removed by filtration and discarded. The filtrate was concentrated under reduced pressure, hexanes (35 mL) were added to the residue, and the flask was once again placed into an ultrasound bath until a homogeneous white precipitate in a pale yellow solution was obtained. The precipitate was removed by filtration, and the filtrate concentrated to yield 1-bromo-1-(4-bromophenyl)-3-(trimethylsilyl)prop-2-yne (**7**) in 89% yield (2.19 g, 6.30 mmol) as a yellow oil. ^{1}H NMR (400.1 MHz $CDCl_3$): δ 0.23 (s, 9 H, $Si(CH_3)_3$, 5.66 (s, 2 H, C*H*Br), 7.43−7.52 (m, 4 H, C_6H_4Br). $^{13}C\{^1H\}$ NMR (175.9 MHz, $CDCl_3$): δ 0.1 ($Si(CH_3)_3$), 36.3 (CHBr), 96.2 (C≡*C*-Si), 101.9 (C≡C−Si), 123.5 (*C*-1, C_6H_4), 129.8 (*C*-2/*C*-6, C_6H_4), 132.5 (*C*-3/*C*-5, C_6H_4), 138.4 (*C*-4, C_6H_4).

A solution of n-butyllithium in hexanes (2.17 mL, 1.6 M, 3.47 mmol of n-BuLi) was added in a single portion to a solution of bis(trimethylsilyl)-amine (510 mg, 3.18 mmol) in tetrahydrofuran (6 mL) at −10 °C. The resulting mixture was stirred for 10 min at −10 °C, followed by addition of hexamethylphosphoric triamide (HMPA, 569 mg, 3.18 mmol). This mixture was taken up in a syringe and added dropwise by means of a mechanical syringe pump (flow rate 75.0 $\mu Lmin^{-1}$) to a solution of **7** (1.00 g, 2.89 mmol) in tetrahydrofuran (12 mL) at −85 °C. Following completion of the addition the mixture was stirred at −85 °C for 10 min before being poured *without warming* onto a mixture of ice (20 g) and saturated aqueous ammonium chloride solution (30 mL). The resulting mixture was allowed to warm to ambient temperature and extracted with diethyl ether (3 × 20 mL), the combined organic extracts were then washed sequentially with cold (0 °C) hydrochloric acid (1 M, 40 mL), water (20 mL), saturated aqueous sodium hydrogen carbonate solution (20 mL), and brine (20 mL), dried over magnesium sulfate, filtered, and concentrated under reduced pressure to afford a brown solid. This solid was purified by column chromatography (eluent: petroleum ether) to yield *E*-**9** in 32% yield (243 mg, 458 μmol) as a white crystalline solid along with a mixture of *E*-**9** and *Z*-**9** in a 1:5 ratio (50%, 381 mg, 718 μmol). *E*/*Z* assignments were confirmed by XRD analysis of a crystal of the *E* isomer (see SI, Figure S5). ^{1}H NMR *E*-isomer (599.8 MHz $CDCl_3$): δ 0.13 (s, 18 H, $Si(CH_3)_3$), 7.48 (δ_A) and 7.72 (δ_B) (AA′BB′ system, $^3J_{A\text{-}B}$ = 8.4 Hz, $^4J_{A\text{-}A',\ B\text{-}B'}$ = 1.4 Hz, 4 H, C_6H_4Br). $^{13}C\{^1H\}$ NMR *E*-isomer (150.8 MHz, $CDCl_3$): δ 0.3 ($Si(CH_3)_3$), 104.5 (C≡*C*−C═C), 106.7 (C≡C−*C*═C), 122.6 (*C*-1, C_6H_4Br), 128.5 (*C*═C), 130.9 (*C*-2/*C*-3/*C*-5/*C*-6, C_6H_4Br), 137.3 (*C*-4, C_6H_4Br). $^{29}Si\{^1H\}$ NMR *E*-isomer (139.0 MHz, $CDCl_3$): δ −17.1. FT-IR (CH_2Cl_2): ν = 1489 (C−H), 2135 (C≡C). EI-MS: m/z (%) 530 (15) $[M^+]$, 73 (100). Anal. calcd for $C_{24}H_{26}Br_2Si_2$: C, 54.34; H, 4.94. Found C, 54.13; H, 5.09. A single crystal of **9** suitable for XRD studies was grown by slow evaporation of a solution in dichloromethane.

*(E)-3,4-Bis(4-bromophenyl)-1,6-bis(tri-isopropylsilyl)hexa-3-en-1,5-diyne (**10**).* Bromine (1.04 g, 6.53 mmol of Br_2) was added dropwise at 0 °C to a stirred solution of triphenylphosphine (1.79 g, 6.81 mmol) in dichloromethane (21 mL). A solution of compound **14** (2.00 g, 5.44 mmol) and imidazole (445 mg, 6.53 mmol) in dichloromethane (7 mL) was added to the solution of bromine triphenylphosphine complex via cannula at 0 °C. Subsequently, the reaction mixture was allowed to warm to ambient temperature, stirred for 3 h at this temperature, and concentrated *in vacuo*. Diethyl ether (20 mL) was added to the residue, and the flask was placed into an ultrasound bath until a homogeneous beige precipitate in a pale yellow solution was obtained. The precipitate was removed by filtration and discarded. The filtrate was concentrated under reduced pressure, hexanes (30 mL) were added to the residue, and the flask was once again placed into an ultrasound bath until a homogeneous white precipitate in a pale yellow solution was obtained. The precipitate was removed by filtration and the filtrate concentrated to yield 1-bromo-1-(4-bromophenyl)-3-(tri-isopropylsilyl)prop-2-yne (**8**) in 98% yield (2.31 g, 5.37 mmol) as a pale yellow oil. ^{1}H NMR (699.7 MHz $CDCl_3$): δ 1.09−1.11 (m, 21 H, $Si(CH(CH_3)_2)_2$), 5.70 (s, 2 H, C*H*Br), 6.00−7.51 (m, 4 H, C_6H_4Br). $^{13}C\{^1H\}$ NMR (175.9 MHz, $CDCl_3$): δ 11.3 ($Si(CH(CH_3)_2)_2$), 18.7 ($Si(CH(CH_3)_2)_2$), 36.2 (CHBr), 93.1 (C≡*C*-Si), 103.5 (C≡C−Si), 123.1 (*C*-1, C_6H_4), 129.5 (*C*-2/*C*-6, C_6H_4), 132.1 (*C*-3/*C*-5, C_6H_4), 138.4 (*C*-4, C_6H_4). $^{29}Si\{^1H\}$ NMR (139.0 MHz, $CDCl_3$): δ −1.1. FT-IR (neat) ν = 2172 (C≡C).

A solution of n-butyllithium in hexanes (2.59 mL, 2.5 M, 6.47 mmol of n-BuLi) was added in a single portion to a solution of bis-(trimethylsilyl)amine (951 mg, 5.93 mmol) in tetrahydrofuran (11 mL) at −10 °C. The resulting mixture was stirred for 20 min at −10 °C followed by addition of hexamethylphosphoric triamide (HMPA, 1.06 g, 5.93 mmol), this mixture was taken up in a syringe and added dropwise by means of a mechanical syringe pump (flow rate 70.0 $\mu Lmin^{-1}$) to a solution of **8** (2.32 g, 5.39 mmol) in tetrahydrofuran (22 mL) at −78 °C. Following completion of the addition the mixture was stirred at −78 °C for 10 min before being poured without warming onto a mixture of ice (20 g) and saturated aqueous ammonium chloride solution (30 mL). The resulting mixture was allowed to warm to ambient temperature and was extracted with diethyl ether (4 × 20 mL). The combined organic extracts were then washed sequentially with cold (0 °C) hydrochloric acid (1 M, 40 mL), water (20 mL), saturated aqueous sodium hydrogen carbonate solution (20 mL) and brine (20 mL), dried over magnesium sulfate, filtered, and concentrated under reduced pressure to afford a pale yellow solid. This solid was recrystallized from boiling ethanol (abs.) to yield **10** in 56% yield as white needles. *E*/*Z* assignments were confirmed by XRD analysis of a crystal of the *E* isomer (see SI, Figure S6). ^{1}H NMR (699.7 MHz $CDCl_3$): δ 0.99−1.01 (m, 42 H, $Si(CH(CH_3)_2)_2$), 7.46 (δ_A) and 7.75 (δ_B) (AA′BB′ system, $^3J_{A\text{-}B}$ = 8.6 Hz, $^4J_{A\text{-}A',\ B\text{-}B'}$ = 1.9 Hz, 8 H, C_6H_4Br). $^{13}C\{^1H\}$ NMR (175.9 MHz, $CDCl_3$): δ 11.4 ($Si(CH(CH_3)_2)_2$), 18.7 ($Si(CH(CH_3)_2)_2$), 103.9 (C≡*C*−C═C), 106.3 (C≡C−*C*═C), 122.4 (*C*-1, C_6H_4Br), 128.7 (*C*═*C*), 130.9 and 131.0 (*C*-2/*C*-3/*C*-5/*C*-6, C_6H_4Br), 137.9 (*C*-4, C_6H_4Br). $^{29}Si\{^1H\}$ NMR (139.0 MHz, $CDCl_3$): δ − 1.7. FT-IR (Nujol) ν = 1461 (C−H), 2125 (C≡C). APCI-MS: m/z (%) 698 (100) $[M^+]$. Anal. calcd for $C_{36}H_{50}Br_2Si_2$: C, 61.88; H, 7.21. Found C, 61.73; H, 7.29. HRMS (ESI-TOF) m/z: $[M]^+$ calcd for $C_{36}H_{50}Br_2Si_2$ 696.1818; Found 696.1811. A single crystal of **10** suitable for XRD studies was grown by slow evaporation of a solution in dichloromethane.

DOI: 10.1021/acs.joc.5b02240
J. Org. Chem. 2015, 80, 11501−11512

1-(4-Bromophenyl)-3-(tri-isopropylsilyl)prop-2-yn-1-ol (**14**). A solution of *n*-butyllithium in hexanes (24.2 mL, 1.6 M, 38.6 mmol of *n*-BuLi) was added in approximately 5 mL portions over a period of 5 min to a solution of 4-bromobenzaldehyde (5.50 g, 29.7 mmol) and **12** (5.96 g, 32.7 mmol) in tetrahydrofuran (50 mL) at −78 °C. The reaction mixture was then stirred for 1 h at −78 °C, allowed to warm to ambient temperature, and stirred for 16 h at this temperature. Subsequently, a saturated aqueous solution of ammonium chloride (50 mL) was added followed by ethyl acetate (30 mL), and the aqueous phase was separated, extracted with ethyl acetate (2 × 30 mL), and discarded. Washing of the combined organic extracts with brine (2 × 50 mL), drying over magnesium sulfate, filtration, and concentration under reduced pressure gave a pale yellow oil. This oil was purified by bulb-to-bulb distillation under reduced pressure (6×10^{-2} mbar, 120−200 °C) to afford **14** in 52% yield (5.75 g, 15.6 mmol) as a colorless, viscous oil. ^{1}H NMR (599.6 MHz $CDCl_3$): δ 1.08−1.09 (m, 21 H, Si(C*H*(C*H*$_3$)$_2$), 7.45 (δ_A) and 7.51 (δ_B) (AA′BB′ system, $^3J_{A-B}$ = 8.2 Hz, $^4J_{A\text{-}A',\,B-B'}$ = 1.9 Hz, 4 H, C_6H_4Br). ^{13}C{^{1}H} NMR (150.8 MHz, $CDCl_3$): δ 11.3 (Si(CH(CH_3)$_2$), 18.7 (Si(CH(CH_3)$_2$), 64.6 (CHOH), 88.7 (C≡*C*-Si), 106.5 (C≡C−Si), 122.5 (C-1, C_6H_4Br), 128.6 (C-2/C-6, C_6H_4Br), 131.8 (C-3/C-5, C_6H_4Br), 139.7 (C-4, C_6H_4Br). ^{29}Si{^{1}H} NMR (139.0 MHz, $CDCl_3$): δ − 1.7. FT-IR (neat) ν = 2170 (C≡C), 3328 (O−H). EI-MS: *m*/*z* (%) 368 (18) [M^+], 325 (22) [M^+ − CH(CH_3)], 267 (100). Anal. calcd for $C_{18}H_{27}OBrSi$: C, 58.85; H, 7.41. Found C, 58.72; H, 7.28.

Computational Details. Structure optimizations as well as bonding analyses were performed with TURBOMOLE 6.4.[62] All DFT calculations reported in the paper were performed with the global hybrid functional BLYP35.[45,46,63,64] This exchange−correlation functional was constructed according to

$$E_{XC} = 0.65(E_X^{LDSA} + \Delta E_X^{B88}) + 0.35E_X^{exact} + E_C^{LYP}$$

While not a thermochemically optimized functional, BLYP35 has been shown to provide good agreement with ground- and excited-state experimental data for organic mixed-valence systems[45,46,64−66] as well as for mixed-valence transition-metal complexes.[63,67,68] Since all experiments were carried out in dichloromethane (permittivity ε = 8.93), it has been modeled by the conductor-like screening solvent model (COSMO)[69] in TURBOMOLE 6.4. For all calculations def2-TZVP basis sets were employed.[70] Spin-density isosurface plots were obtained with the Molekel program.[71]

Subsequent TDDFT calculations of the lowest-energy electronic transitions (IVCT bands) were done with the Gaussian 09 program,[72] using the same functional and basis sets.[70] In the Gaussian 09 calculations, solvent effects have been included by the CPCM keyword,[73] which denotes the polarizable continuum model that is closest to the COSMO model used in the optimizations. TURBOMOLE 6.4 was also used for TDDFT calculations. However, the Gaussian 09 results for **1** and **3** were consistently closer to experiment (differences are due to cavity construction and, in particular, treatment of nonequilibrium solvation in the two codes). Therefore, only these results are reported here.

■ ASSOCIATED CONTENT

Supporting Information

The Supporting Information is available free of charge on the ACS Publications website at DOI: 10.1021/acs.joc.5b02240.

^{1}H (**1**−**6**, *E*-**9**, **10**, **14**) and ^{13}C (**2**−**6**, *E*-**9**, **10**, **14**) NMR spectra; UV−vis spectra of **1** and **3** in solvent mixtures of differing polarity, details of XRD studies on **1**, **6**, *E*-**9**, and **10**; full range IR spectra of $[\mathbf{1}]^{n+}$ and $[\mathbf{3}]^{n+}$; UV−vis spectrum of **16**; computational details and optimized coordinates in XYZ format for **1**, **3** and $[\mathbf{1}']^+$. Additionally all crystallographic data (excluding structure factors) for the structures reported herein have been deposited with The Cambridge Crystallographic Data Centre as supplementary publication nos. CCDC-1047238 (**1**), CCDC-1047239 (**6**), CCDC-1047240 (*E*-**9**), and CCDC-1047241 (**10**). Copies of these data can be obtained free of charge via www.ccdc.cam.ac.uk/data_request/cif (PDF)

CIF files of **1**, **6**, *E*-**9**, and **10** (CIF)

(XYZ)

■ AUTHOR INFORMATION

Corresponding Author

*E-mail: paul.low@uwa.edu.au. Phone: +61-8-6488-3045

Notes

The authors declare no competing financial interest.

■ ACKNOWLEDGMENTS

This research was supported by the EPSRC and the ARC (DP 140100855). J.B.G.G. thanks Prof. P. G. Steel, Prof. M. R. Bryce, Dr. P. W. Dyer, Dr. M. A. Fox, and their respective research groups for the loan of equipment and chemicals that greatly enhanced this project. P.J.L. held an EPSRC Leadership Fellowship and now holds an ARC Future Fellowship (FT 120100073). Work in Berlin was supported by DFG project KA1187/13-1.

■ REFERENCES

(1) Gholami, M.; Tykwinski, R. R. *Chem. Rev.* **2006**, *106*, 4997−5027.
(2) Opsitnick, E.; Lee, D. *Chem. - Eur. J.* **2007**, *13*, 7040−7049.
(3) Zucchero, A. J.; McGrier, P. L.; Bunz, U. H. F. *Acc. Chem. Res.* **2010**, *43*, 397−408.
(4) Saeed, M. A.; Le, H. T. M.; Miljanić, O. Š. *Acc. Chem. Res.* **2014**, *47*, 2074−2083.
(5) Saragi, T. P. I.; Spehr, T.; Siebert, A.; Fuhrmann-Lieker, T.; Salbeck, J. *Chem. Rev.* **2007**, *107*, 1011−1065.
(6) Shirota, Y.; Kageyama, H. *Chem. Rev.* **2007**, *107*, 953−1010.
(7) Nielsen, M. B.; Diederich, F. *Chem. Rev.* **2005**, *105*, 1837−1868.
(8) Kivala, M.; Diederich, F. *Acc. Chem. Res.* **2009**, *42*, 235−248.
(9) Marsden, J. A.; Miller, J. J.; Shirtcliff, L. D.; Haley, M. M. *J. Am. Chem. Soc.* **2005**, *127*, 2464−2476.
(10) Dalton, G. T.; Cifuentes, M. P.; Petrie, S.; Stranger, R.; Humphrey, M. G.; Samoc, M. *J. Am. Chem. Soc.* **2007**, *129*, 11882−11883.
(11) Ito, S.; Akimoto, K.; Kawakami, J.; Tajiri, A.; Shoji, T.; Satake, H.; Morita, N. *J. Org. Chem.* **2007**, *72*, 162−172.
(12) Nithya, R.; Senthilkumar, K. *Org. Electron.* **2014**, *15*, 1607−1623.
(13) Shin, J.; Kang, N. S.; Lee, T. W.; Cho, M. J.; Hong, J. M.; Ju, B.-K.; Choi, D. H. *Org. Electron.* **2014**, *15*, 1521−1530.
(14) Kiguchi, M.; Takahashi, Y.; Fujii, S.; Takase, M.; Narita, T.; Iyoda, M.; Horikawa, M.; Naitoh, Y.; Nakamura, H. *J. Phys. Chem. C* **2014**, *118*, 5275−5283.
(15) Broman, S. L.; Nielsen, M. B. *Phys. Chem. Chem. Phys.* **2014**, *16*, 21172−21182.
(16) Parker, C. R.; Leary, E.; Frisenda, R.; Wei, Z.; Jennum, K. S.; Glibstrup, E.; Abrahamsen, P. B.; Santella, M.; Christensen, M. A.; Pia; Della, E. A.; Li, T.; González, M. T.; Jiang, X.; Morsing, T. J.; Rubio-Bollinger, G.; Laursen, B. W.; Nørgaard, K.; van der Zant, H.; Agraït, N.; Nielsen, M. B. *J. Am. Chem. Soc.* **2014**, *136*, 16497−16507.
(17) Fjelbye, K.; Christensen, T. N.; Jevric, M.; Broman, S. L.; Petersen, A. U.; Kadziola, A.; Nielsen, M. B. *Eur. J. Org. Chem.* **2014**, *2014*, 7859−7864.
(18) Baghernejad, M.; Zhao, X.; Baruël Ørnsø, K.; Füeg, M.; Moreno-García, P.; Rudnev, A. V.; Kaliginedi, V.; Vesztergom, S.; Huang, C.; Hong, W.; Broekmann, P.; Wandlowski, T.; Thygesen, K. S.; Bryce, M. R. *J. Am. Chem. Soc.* **2014**, *136*, 17922−17925.
(19) Zhao, Y.; Lindsay, S.; Jeon, S.; Kim, H.-J.; Su, L.; Lim, B.; Koo, S. *Chem. - Eur. J.* **2013**, *19*, 10832−10835.

DOI: 10.1021/acs.joc.5b02240
J. Org. Chem. 2015, 80, 11501−11512

(20) Guédon, C. M.; Valkenier, H.; Markussen, T.; Thygesen, K. S.; Hummelen, J. C.; van der Molen, S. J. *Nat. Nanotechnol.* **2012**, *7*, 305−309.
(21) Valkenier, H.; Guédon, C. M.; Markussen, T.; Thygesen, K. S.; van der Molen, S. J.; Hummelen, J. C. *Phys. Chem. Chem. Phys.* **2014**, *16*, 653−662.
(22) Kaliginedi, V.; Moreno-García, P.; Valkenier, H.; Hong, W.; García-Suárez, V. M.; Buiter, P.; Otten, J. L. H.; Hummelen, J. C.; Lambert, C. J.; Wandlowski, T. *J. Am. Chem. Soc.* **2012**, *134*, 5262−5275.
(23) Kocherzhenko, A. A.; Siebbeles, L. D. A.; Grozema, F. C. *J. Phys. Chem. Lett.* **2011**, *2*, 1753−1756.
(24) Jones, G. B.; Wright, J. M.; Plourde, G. W.; Hynd, G.; Huber, R. S.; Mathews, J. E. *J. Am. Chem. Soc.* **2000**, *122*, 1937−1944.
(25) Horino, Y.; Homura, N.; Inoue, K.; Yoshikawa, S. *Adv. Synth. Catal.* **2012**, *354*, 828−834.
(26) Wolfe, J. P.; Tomori, H.; Sadighi, J. P.; Yin, J.; Buchwald, S. L. *J. Org. Chem.* **2000**, *65*, 1158−1174.
(27) Surry, D. S.; Buchwald, S. L. *Chem. Sci.* **2011**, *2*, 27−50.
(28) Onitsuka, K.; Ohara, N.; Takei, F.; Takahashi, S. *Dalton Trans.* **2006**, 3693−3698.
(29) Sonogashira, K.; Tohda, Y.; Hagihara, N. *Tetrahedron Lett.* **1975**, *16*, 4467−4470.
(30) Sonogashira, K. *J. Organomet. Chem.* **2002**, *653*, 46−49.
(31) Chinchilla, R.; Najera, C. *Chem. Rev.* **2007**, *107*, 874−922.
(32) Marqués-González, S.; Yufit, D. S.; Howard, J. A. K.; Martín, S.; Osorio, H. M.; García-Suárez, V. M.; Nichols, R. J.; Higgins, S. J.; Cea, P.; Low, P. J. *Dalton Trans.* **2012**, *42*, 338−341.
(33) Pera, G.; Martín, S.; Ballesteros, L. M.; Hope, A. J.; Low, P. J.; Nichols, R. J.; Cea, P. *Chem. - Eur. J.* **2010**, *16*, 13398−13405.
(34) Wang, C.; Batsanov, A. S.; Bryce, M. R.; Martín, S.; Nichols, R. J.; Higgins, S. J.; García-Suárez, V. M.; Lambert, C. J. *J. Am. Chem. Soc.* **2009**, *131*, 15647−15654.
(35) Kamenetska, M.; Quek, S. Y.; Whalley, A. C.; Steigerwald, M. L.; Choi, H. J.; Louie, S. G.; Nuckolls, C.; Hybertsen, M. S.; Neaton, J. B.; Venkataraman, L. *J. Am. Chem. Soc.* **2010**, *132*, 6817−6821.
(36) Tam, E. S.; Parks, J. J.; Shum, W. W.; Zhong, Y.-W.; Santiago-Berríos, M. B.; Zheng, X.; Yang, W.; Chan, G. K. L.; Abruña, H. D.; Ralph, D. C. *ACS Nano* **2011**, *5*, 5115−5123.
(37) Reger, D. L.; Gardinier, J. R.; Smith, M. D.; Shahin, A. M.; Long, G. J.; Rebbouh, L.; Grandjean, F. *Inorg. Chem.* **2005**, *44*, 1852−1866.
(38) Heckmann, A.; Lambert, C. *Angew. Chem., Int. Ed.* **2012**, *51*, 326−392.
(39) Connelly, N. G.; Geiger, W. E. *Chem. Rev.* **1996**, *96*, 877−910.
(40) Barlow, S.; Risko, C.; Coropceanu, V.; Tucker, N. M.; Jones, S. C.; Levi, Z.; Khrustalev, V. N.; Antipin, M. Y.; Kinnibrugh, T. L.; Timofeeva, T.; Marder, S. R.; Brédas, J.-L. *Chem. Commun.* **2005**, 764−766.
(41) Barlow, S.; Risko, C.; Chung, S.-J.; Tucker, N. M.; Coropceanu, V.; Jones, S. C.; Levi, Z.; Brédas, J.-L.; Marder, S. R. *J. Am. Chem. Soc.* **2005**, *127*, 16900−16911.
(42) Winter, R. F. *Organometallics* **2014**, *33*, 4517−4536.
(43) Low, P. J.; Brown, N. J. *J. Cluster Sci.* **2010**, *21*, 235−278.
(44) D'Alessandro, D. M.; Keene, F. R. *Dalton Trans.* **2004**, 3950−3954.
(45) Renz, M.; Theilacker, K.; Lambert, C.; Kaupp, M. *J. Am. Chem. Soc.* **2009**, *131*, 16292−16302.
(46) Kaupp, M.; Renz, M.; Parthey, M.; Stolte, M.; Würthner, F.; Lambert, C. *Phys. Chem. Chem. Phys.* **2011**, *13*, 16973.
(47) Liu, Z.-Q.; Fang, Q.; Cao, D.-X.; Wang, D.; Xu, G.-B. *Org. Lett.* **2004**, *6*, 2933−2936.
(48) Xia, C.; Wang, X.; Lin, J.; Jiang, W.; Ni, Y.; Huang, W. *Synth. Met.* **2009**, *159*, 194−200.
(49) Sugiyama, Y.; Shinohara, Y.; Momotake, A.; Takahashi, K.; Kanna, Y.; Nishimura, Y.; Arai, T. *J. Phys. Chem. A* **2010**, *114*, 10929−10935.
(50) Kondrasenko, I.; Kisel, K. S.; Karttunen, A. J.; Jänis, J.; Grachova, E. V.; Tunik, S. P.; Koshevoy, I. O. *Eur. J. Inorg. Chem.* **2015**, *2015*, 864−875.
(51) Berenguer, J. R.; Fernández, J.; Gil, B.; Lalinde, E.; Sánchez, S. *Chem. - Eur. J.* **2014**, *20*, 2574−2584.
(52) Xiang, J.; Wu, J.-S. *Z. Anorg. Allg. Chem.* **2013**, *639*, 606−610.
(53) Hinderer, F.; Bunz, U. H. F. *Chem. - Eur. J.* **2013**, *19*, 8490−8496.
(54) Krejčik, M.; Daněk, M.; Hartl, F. J. *J. Electroanal. Chem. Interfacial Electrochem.* **1991**, *317*, 179−187.
(55) Mihigo, S. O.; Mammo, W.; Bezabih, M.; Andrae-Marobela, K.; Abegaz, B. M. *Bioorg. Med. Chem.* **2010**, *18*, 2464−2473.
(56) Fairlamb, I. J. S.; Kapdi, A. R.; Lee, A. F. *Org. Lett.* **2004**, *6*, 4435−4438.
(57) Bureš, F.; Čermáková, H.; Kulhánek, J.; Ludwig, M.; Kuznik, W.; Kityk, I. V.; Mikysek, T.; Růžička, A. *Eur. J. Org. Chem.* **2012**, *2012*, 529−538.
(58) Zhao, X.; Huang, C.; Gulcur, M.; Batsanov, A. S.; Baghernejad, M.; Hong, W.; Bryce, M. R.; Wandlowski, T. *Chem. Mater.* **2013**, *25*, 4340−4347.
(59) Kauffman, J. M.; Moyna, G. *J. Org. Chem.* **2003**, *68*, 839−853.
(60) Fulmer, G. R.; Miller, A. J. M.; Sherden, N. H.; Gottlieb, H. E.; Nudelman, A.; Stoltz, B. M.; Bercaw, J. E.; Goldberg, K. I. *Organometallics* **2010**, *29*, 2176−2179.
(61) Gluyas, J. B. G.; Boden, A. J.; Eaves, S. G.; Yu, H.; Low, P. J. *Dalton Trans.* **2014**, *43*, 6291−6294.
(62) *TURBOMOLE*; Turbomole GmbH: A development of University of Karlsruhe and Forschungszentrum Karlsruhe GmbH: Karlsruhe, Germany, 1989−2007, 2012.
(63) Parthey, M.; Kaupp, M. *Chem. Soc. Rev.* **2014**, *43*, 5067−5088.
(64) Renz, M.; Kess, M.; Diedenhofen, M.; Klamt, A.; Kaupp, M. *J. Chem. Theory Comput.* **2012**, *8*, 4189−4203.
(65) Renz, M.; Kaupp, M. *J. Phys. Chem. A* **2012**, *116*, 10629−10637.
(66) Völker, S. F.; Renz, M.; Kaupp, M.; Lambert, C. *Chem. - Eur. J.* **2011**, *17*, 14147−14163.
(67) Parthey, M.; Gluyas, J. B. G.; Fox, M. A.; Low, P. J.; Kaupp, M. *Chem. - Eur. J.* **2014**, *20*, 6895−6908.
(68) Parthey, M.; Gluyas, J. B. G.; Schauer, P. A.; Yufit, D. S.; Howard, J. A. K.; Kaupp, M.; Low, P. J. *Chem. - Eur. J.* **2013**, *19*, 9780−9784.
(69) Klamt, A.; Schüürmann, G. *J. Chem. Soc., Perkin Trans. 2* **1993**, 799.
(70) Weigend, F.; Häser, M.; Patzelt, H.; Ahlrichs, R. *Chem. Phys. Lett.* **1998**, *294*, 143−152.
(71) Varetto, U. *MOLEKEL 5.4*; Swiss National Computing Centre, Manno, Switzerland.
(72) Frisch, M. J.; Trucks, G. W.; Schlegel, H. B.; Scuseria, G. E.; Robb, M. A.; Cheeseman, J. R.; Scalmani, G.; Barone, V.; Mennucci, B.; Petersson, G. A.; Nakatsuji, H.; Caricato, M.; Li, X.; Hratchian, H. P.; Izmaylov, A. F.; Bloino, J.; Zheng, G.; Sonnenberg, J. L.; Hada, M.; Ehara, M.; Toyota, K.; Fukuda, R.; Hasegawa, J.; Ishida, M.; Nakajima, T.; Honda, Y.; Kitao, O.; Nakai, H.; Vreven, T.; Montgomery, J. A., Jr.; Peralta, J. E.; Ogliaro, F.; Bearpark, M. J.; Heyd, J.; Brothers, E. N.; Kudin, K. N.; Staroverov, V. N.; Kobayashi, R.; Normand, J.; Raghavachari, K.; Rendell, A. P.; Burant, J. C.; Iyengar, S. S.; Tomasi, J.; Cossi, M.; Rega, N.; Millam, N. J.; Klene, M.; Knox, J. E.; Cross, J. B.; Bakken, V.; Adamo, C.; Jaramillo, J.; Gomperts, R.; Stratmann, R. E.; Yazyev, O.; Austin, A. J.; Cammi, R.; Pomelli, C.; Ochterski, J. W.; Martin, R. L.; Morokuma, K.; Zakrzewski, V. G.; Voth, G. A.; Salvador, P.; Dannenberg, J. J.; Dapprich, S.; Daniels, A. D.; Farkas, Ö.; Foresman, J. B.; Ortiz, J. V.; Cioslowski, J.; Fox, D. J. *Gaussian 09*, Gaussian, Inc.: Wallingford, CT, 2009.
(73) Barone, V.; Cossi, M. *J. Phys. Chem. A* **1998**, *102*, 1995−2001.

DOI: 10.1021/acs.joc.5b02240
J. Org. Chem. 2015, 80, 11501−11512